FACIES, DEPOSITIONAL ENVIRONMENTS, AND RESERVOIR PROPERTIES OF THE SHATTUCK SANDSTONE, MESA QUEEN FIELD AND SURROUNDING AREAS, SOUTHEASTERN NEW MEXICO

A Thesis

by

JARED BRANDON HAIGHT

Submitted to the Office of Graduate Studies of
Texas A&M University
in partial fulfillment of the requirements for the degree of

MASTER OF SCIENCE

August 2002

Major Subject: Geology

FACIES, DEPOSITIONAL ENVIRONMENTS, AND RESERVOIR PROPERTIES OF THE SHATTUCK SANDSTONE, MESA QUEEN FIELD AND SURROUNDING AREAS, SOUTHEASTERN NEW MEXICO

A Thesis

by

JARED BRANDON HAIGHT

Submitted to Texas A&M University
in partial fulfillment of the requirements
for the degree of

MASTER OF SCIENCE

Approved as to style and content by:

Brian J. Willis (Chair of Committee)	Thomas A. Blasingame (Member)
Wayne M. Ahr (Member)	Andrew Hajash, Jr. (Head of Department)

August 2002

Major Subject: Geology

ABSTRACT

Facies, Depositional Environments, and Reservoir Properties of the Shattuck Sandstone, Mesa Queen Field and Surrounding Areas, Southeastern New Mexico.

(August 2002)

Jared Brandon Haight, B.S., The University of Oklahoma

Chair of Advisory Committee: Dr. Brian J. Willis

The Shattuck Sandstone Member of the Guadalupian age Queen Formation was deposited in back-reef environments on a carbonate platform of the Northwest Shelf (Permian Basin, New Mexico, USA) during a lowstand of sea level. At Mesa Queen Field, the Shattuck Sandstone is a sheet-like sand body that averages 30 ft (9.1 m) in thickness. The Shattuck Sandstone includes deposits of four major siliciclastic environments: (1) fluvial sandflats, (2) eolian sand sheets, (3) inland sabkhas, and (4) marine-reworked eolian sands. Fluvial sandflat deposits are further subdivided into sheetflood, wadi plain, and river-mouth deposits. Dolomites, evaporites, and siliciclastics that formed in adjacent coastal sabkha and lagoonal environments bound the Shattuck Sandstone from above and below.

The Shattuck Sandstone is moderately- to well-sorted, very fine-grained subarkose, with a mean grain size of 98 μm (3.55ϕ). Eolian sand sheet, wadi plain, and marine-reworked eolian facies comprise the productive reservoir intervals. Reservoir quality reflects intragranular and intergranular secondary porosity formed by partial dissolution of labile feldspar grains, and pore-filling anhydrite and dolomite cements.

Vertical successions and regional facies patterns support previous interpretations that these deposits formed during a sea-level lowstand and early stages of the subsequent transgression. Facies patterns across the shelf indicate fluvial sandflats prograded over coastal and continental sabkhas, and eolian sand deposition became more common during sea-level fall and lowstand. During subsequent transgression, eolian sediments in the upper portion of the Shattuck Sandstone were reworked as coastal and lagoon environments became reestablished on the inner carbonate platform.

ACKNOWLEDGMENTS

I would like to sincerely thank Dr. Brian Willis for his constructive criticism and guidance through the later portion of this project. Without his leadership, the completion of this project would not have been possible. I also wish to thank Dr. Jim Mazzullo for his financial support, guidance, and insight during the initial portion of this study. In addition, I would like to thank Dr. Wayne Ahr and Dr. Tom Blasingame for reviewing the manuscript and providing assistance when needed.

I would like to thank my many friends at A&M for their support and friendship throughout graduate school. I also thank Bo Slone, John Layman, and Changsu Ryu for providing assistance with editing and lending their technical expertise when possible.

Finally, I wish to thank my family for their support and encouragement throughout my academic career.

TABLE OF CONTENTS

Page

Page

LIST OF FIGURES

FIGURE Page

LIST OF TABLES

INTRODUCTION

The Shattuck Sandstone Member of the Queen Formation (Permian, Guadalupian) is a major producing horizon on the Northwest Shelf of the Permian Basin (Fig. 1). The Queen, one of five formations of the Artesia Group (Fig. 2), is a diverse series of carbonates, siliciclastics, and evaporites that was deposited in back-reef environments of the Permian Basin. By 1980, three formations of the Artesia Group (Queen, Seven Rivers, and Yates) had produced over 1.3 billion barrels of oil, which illustrates the importance of understanding these back-reef deposits (Ward et al., 1986).

Carbonates and evaporites of the Artesia Group are generally accepted to be intertidal to shallow marine deposits formed during highstands of sea level. The depositional origin of siliciclastic strata, however, has been controversial. Previous studies focused on determining depositional environments of these siliciclastic deposits and their relation to sea-level change. Some studies suggested they formed in shallow marine environments during constant or highstands of sea level (Ball et al., 1971; Pray, 1977; Wheeler, 1989), whereas others have concluded they are deposits formed during sea-level lowstands (Silver and Todd, 1969; Meissner, 1974; Malicse and Mazzullo, 1990, Mazzullo et al., 1991; Andreason, 1992). The lowstand-highstand dilemma of interpreting siliciclastic units within mixed siliciclastic-carbonate systems similar to the Artesia Group is one that is worldwide (Dott and Byers, 1981; Dott et al., 1986).

The environmental interpretation of the Shattuck Sandstone of the Northwest Shelf has been addressed by several previous studies (Malicse and Mazzullo, 1990;

This thesis follows the style and format of the American Association of Petroleum Geologists Bulletin.

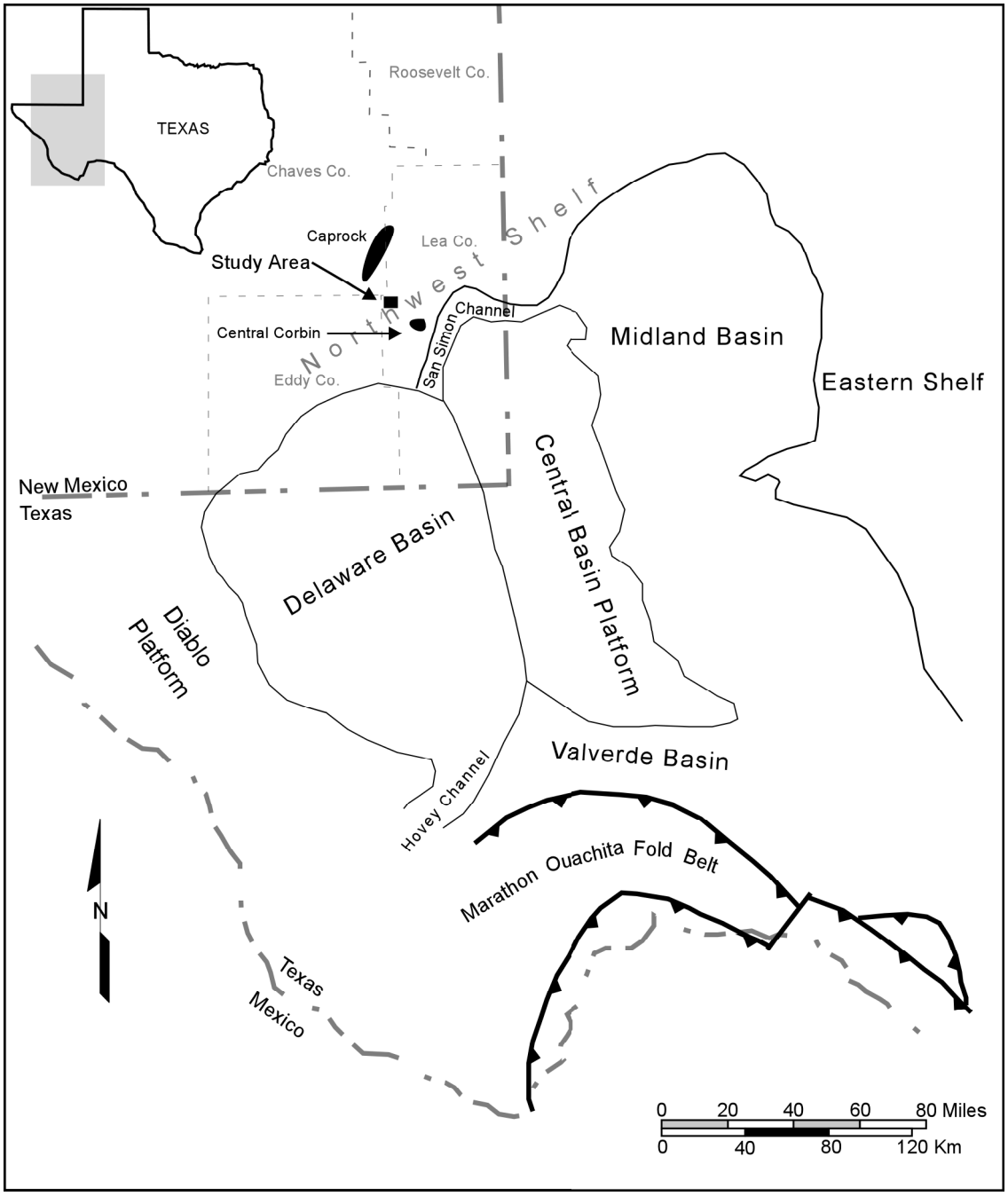

Figure 1. Index map showing the major structural features within the Permian Basin area (Modified from Hills, 1984).

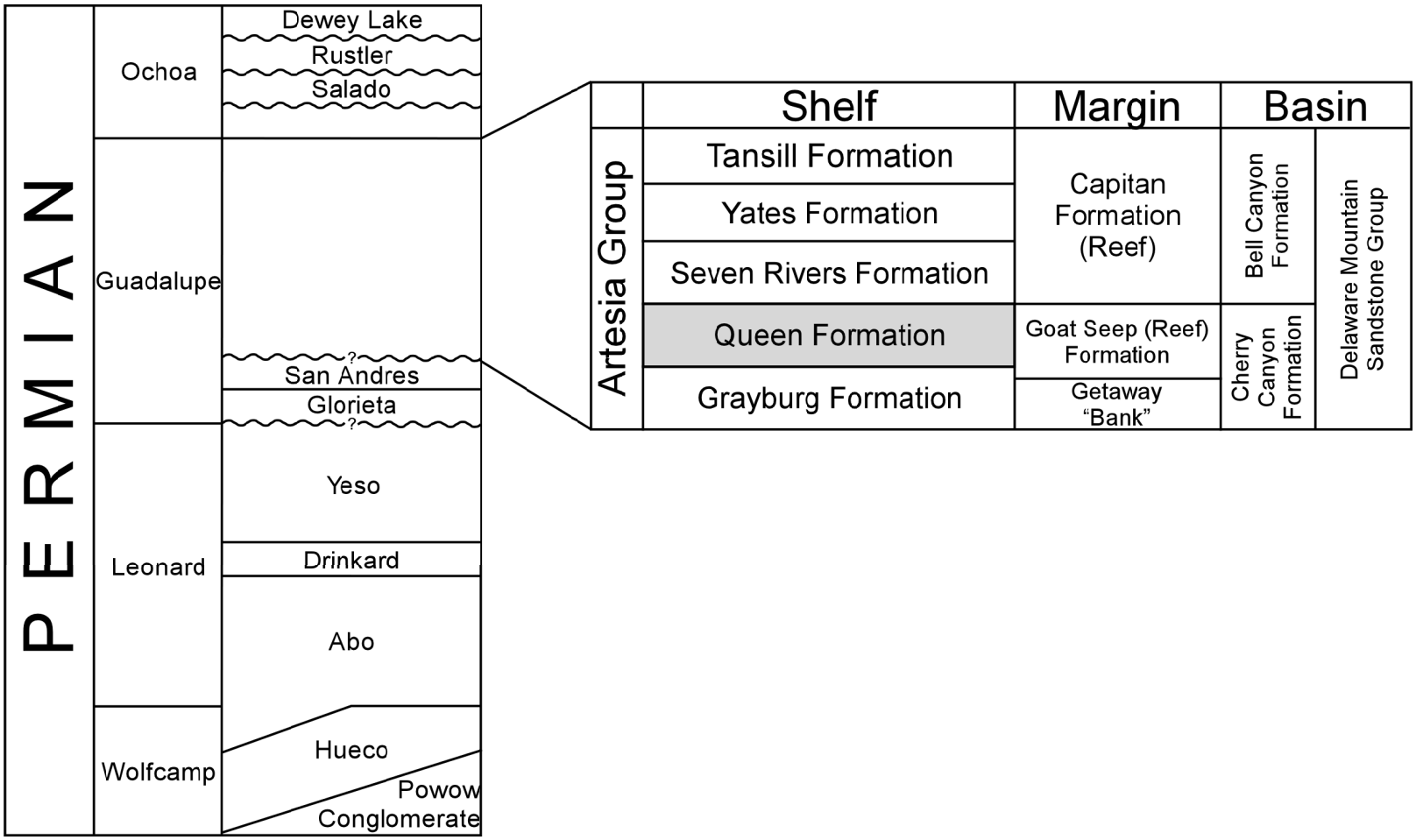

Figure 2. Permian stratigraphy of the Northwest Shelf (Modified from AAPG, 1983c).

Mazzullo et al., 1991). These studies concluded that the Shattuck Sandstone is continental deposits formed in three desert environments: siliciclastic-dominated sabkhas, eolian sand sheets, and fluvial sandflats (Malicse and Mazzullo, 1990; Mazzullo et al., 1991). These isolated field studies also showed that the Shattuck Sandstone formed during a sea-level lowstand, and illustrated the importance of desert fluvial systems in this shelf setting. Less is known about how these depositional systems change spatially across the shelf.

This study examines the Shattuck Sandstone at Mesa Queen Field in Lea County, New Mexico (Fig. 1) to interpret depositional environments, stratigraphy, diagenetic history, and reservoir properties. This detailed reservoir characterization of the Shattuck Sandstone is compared with the previous studies of the Shattuck Sandstone in two adjacent Queen fields - South Caprock (Malicse, 1988) and Central Corbin (Siegel, 1989; Fig. 1). Interpretations of these three fields are compared to define lateral and vertical changes in the facies, broader trends of depositional environments, and associated rock property variations of the Shattuck Sandstone. This study provides a broader record of the represented shelf environments to extend local reservoir characterization studies into a more regional context.

STUDY AREA

Regional Geologic History

The Permian Basin spans 115,000 mi^2 (390,000 km^2) of west Texas and southeast New Mexico. It is comprised of three sub-basins, the Delaware, Midland, and Val Verde; each formed in the foreland of the Marathon-Ouachita orogenic belt (Yang and Dorobek, 1995a).

During the Early Cambrian, the Permian Basin area was a broad, shallow depression called the Tabosa Basin (Galley, 1958; Hills, 1972; Hills, 1985). During this time, deposition was dominated by shallow-water shelf carbonates and siliciclastic muds. Following formation of the Tobosa Basin, little tectonic activity occurred in the region until the start of the Marathon-Ouachita orogeny in the late Mississippian (Hills, 1972). This major tectonic event, resulting from the collision between Laurasia and Gondwanaland, persisted until the Early Permian (Wolfcampian). This tectonism created the main geologic structures in the Permian Basin.

Early Pennsylvanian folds in the central part of the Tobosa Basin formed the Central Basin Uplift. This uplift divided the Permian Basin area into three smaller sub-basins, the Delaware, Midland, and Val Verde (Fig. 1). During this time, siliciclastic mud was deposited in the central parts of the sub-basins, while carbonate reef deposition occurred on shelves rimming the sub-basins (Hills, 1972). Increased tectonism during the Early Pennsylvanian uplifted mountain ranges in the Central Basin Uplift (Hills, 1972). Tectonic activity decreased by the Early Permian, and reef formation along the

shelf-edges of the Permian Basin continued. In the Late Permian, the back-reef environments were filled with the complex series of carbonates, siliciclastics, and evaporites that comprise the Artesia Group.

Stratigraphy

The Artesia Group, as first proposed by the Roswell Geological Society (1962), included all Permian Basin shelf rocks located stratigraphically above the San Andres Formation and stratigraphically below the Ochoan Series (Tait et al., 1962). The Artesia Group consists of (in ascending order) the Grayburg, Queen, Seven Rivers, Yates, and Tansill Formations. These formations comprise back-reef facies of the Goat Seep and Capitan Reef complexes that surrounded the Delaware Basin during the Guadalupian (Fig. 3).

The name Queen was first used by Crandall (1929) to describe a section of the strata in the Guadalupe Mountains. A type section was later proposed by Moran (1954) when he described the formation in the Guadalupe Mountains two miles south of the Queen Post Office (Tait et al., 1962). At this location, the Queen is 420 feet thick and is composed largely of anhydrite and sandstone with few interbeds of shale and dolomite. The Shattuck Sandstone is the uppermost sandstone member of the Queen, and has an average thickness of 30 feet at the type locality.

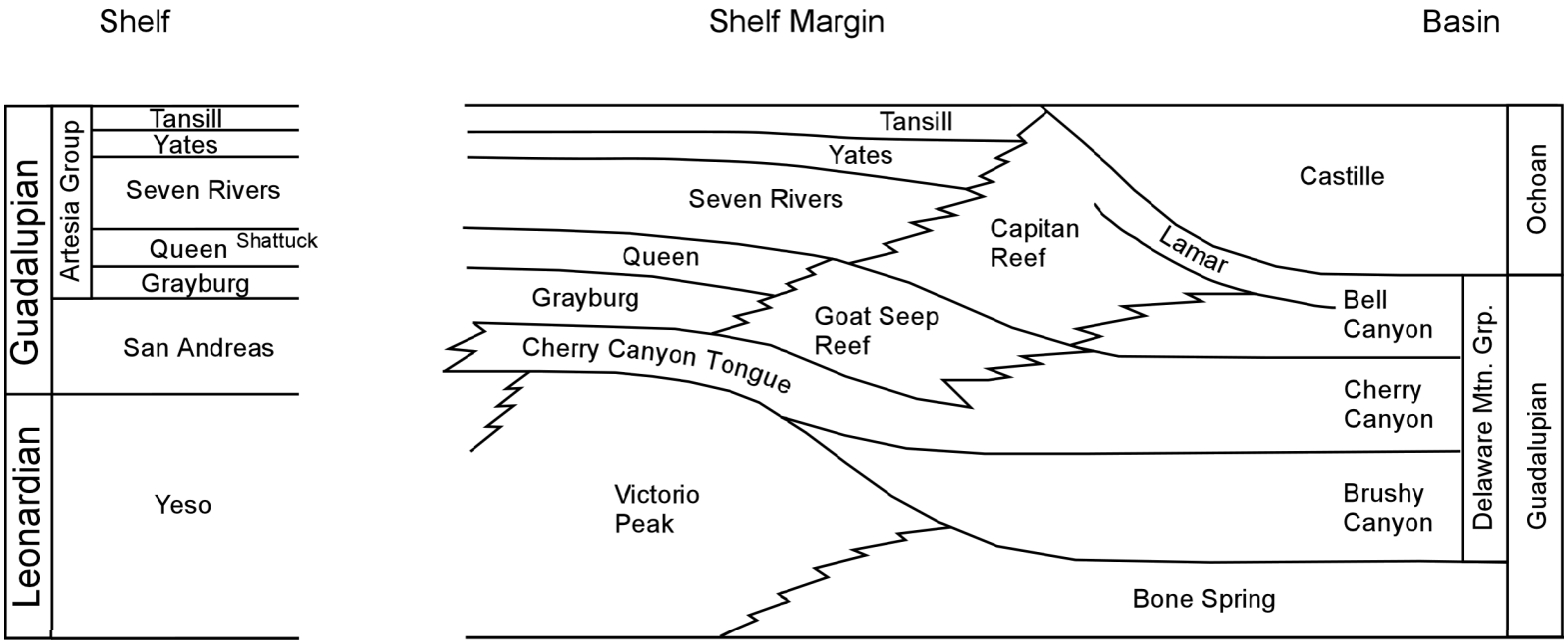

Figure 3. Diagrammatic cross section showing correlations and relationships of stratigraphic units from the Northwest Shelf to the Delaware Basin (Modified after Ward et al., 1986).

DATA AND METHODS

Phase 1 of this study was the geologic characterization of Mesa Queen Field. This was carried out by the examination of seven slabbed, 3.5 inch (8.9 cm) cores obtained from the Texas Bureau of Economic Geology, petrographic analysis of thin sections cut from the core, and the construction of a structural contour and isopach map from well logs (Fig. 4).

The cores were described in detail for lithology, texture, color (based on the Munsell Color Chart), fossil content, sedimentary structures, contacts, and hydrocarbon shows. From these cores, 56 oriented thin sections were cut in a manner to adequately test all sandstone facies present in the Shattuck Sandstone. The thin sections were stained for potassium feldspars with sodium cobaltinitrite to easily distinguish the quartz from the feldspars. The samples were also impregnated with blue epoxy resin to enhance porosity identification. Cores for which only a third of the full core had been preserved were not sampled in order to preserve the sedimentary record. Two-thirds of the full core was preserved in the majority of cases, and in these cases thin sections could be cut from the backside without destroying the slabbed face of the core.

Petrographic analysis was performed on the thin sections to determine grain size, composition, and porosity. Grain size was measured using Image-Pro® Plus digital image analysis software, wherein the long axes of 200 detrital quartz grains were measured for each thin section. The Glagolev-Chayes method was used in the point-counting process to determine composition and porosity (Chayes, 1949; Glagolev, 1934). This method involves the counting of grains in a series of line traverses with the

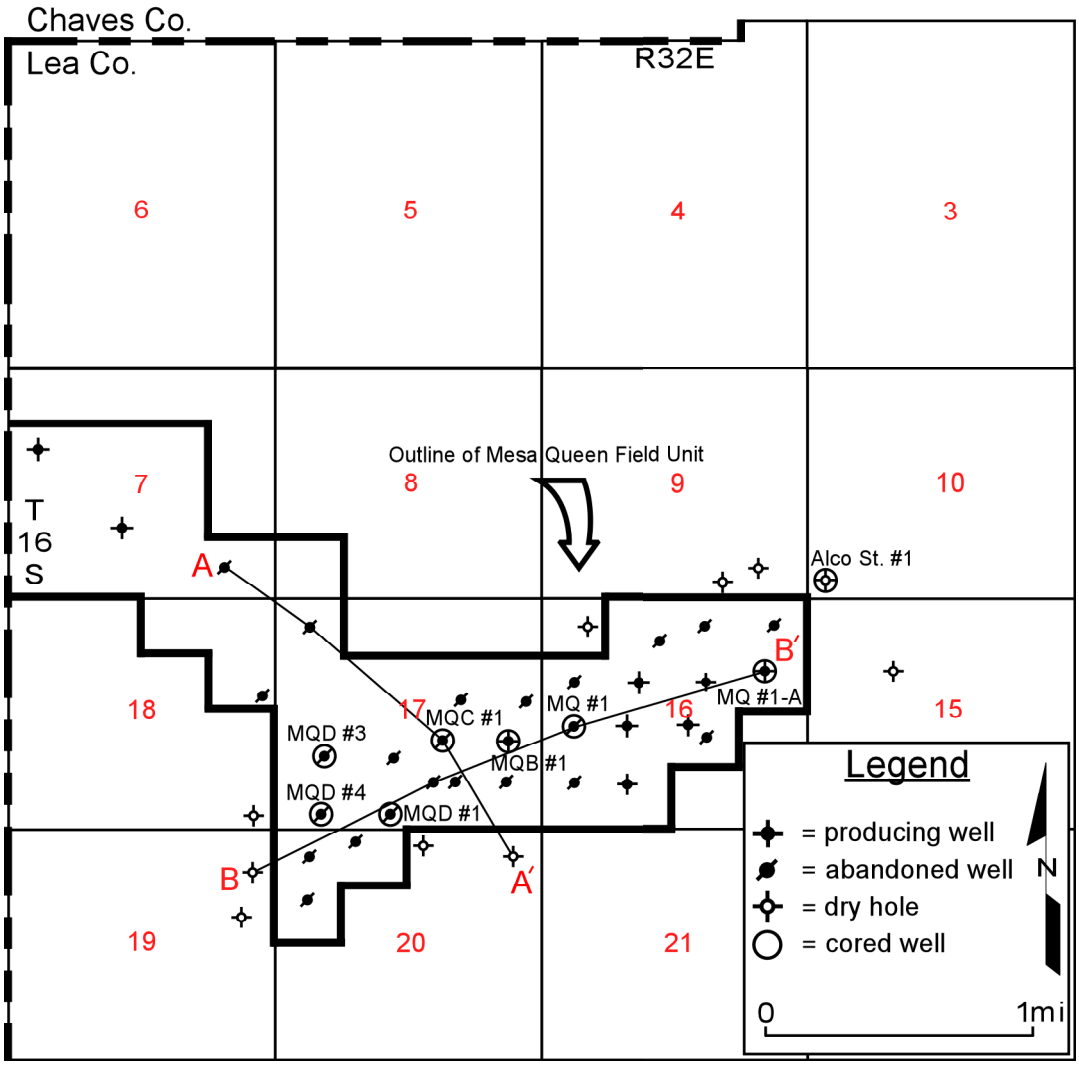

Figure 4. Base map of Mesa Queen Field showing well locations and cored wells.

aid of a graduated mechanical stage. Counting stopped once 100 monocrystalline quartz grains were counted for each thin section. A cut-off value of 100 is sufficient to achieve an acceptable degree of reliability (95% confidence level).

In addition to core and thin section analyses, 36 well logs from Mesa Queen Field and the immediate surrounding area were analyzed to further evaluate the character of the Shattuck Sandstone. The logs consisted of gamma-ray, resistivity, and sonic logs. Gamma-ray logs are best suited to identify the Shattuck Sandstone because of its high radioactivity (Fig. 5).

Well logs were used to estimate gross thickness changes of the Shattuck Sandstone across the study area. An isopach map was constructed to illustrate the geometry of the Shattuck Sandstone. Well logs were also used to construct a structural contour map to further evaluate the geometry of the Shattuck Sandstone.

Phase 2 of this project, was a regional characterization of the Shattuck Sandstone on the Northwest Shelf. This involved comparison of data and interpretations from this study with those from two other studies of nearby Queen fields: South Caprock Field (Malicse, 1988) and Central Corbin Field (Siegel, 1989). Both previous studies provided core descriptions and petrographic analysis of facies within the Shattuck Sandstone. Sand-body geometry, structure, facies and their interpreted depositional environments, grain size, diagenetic and reservoir properties observed in all three fields were collectively compared to produce a broader depositional interpretation of the Shattuck Sandstone on the Northwest Shelf.

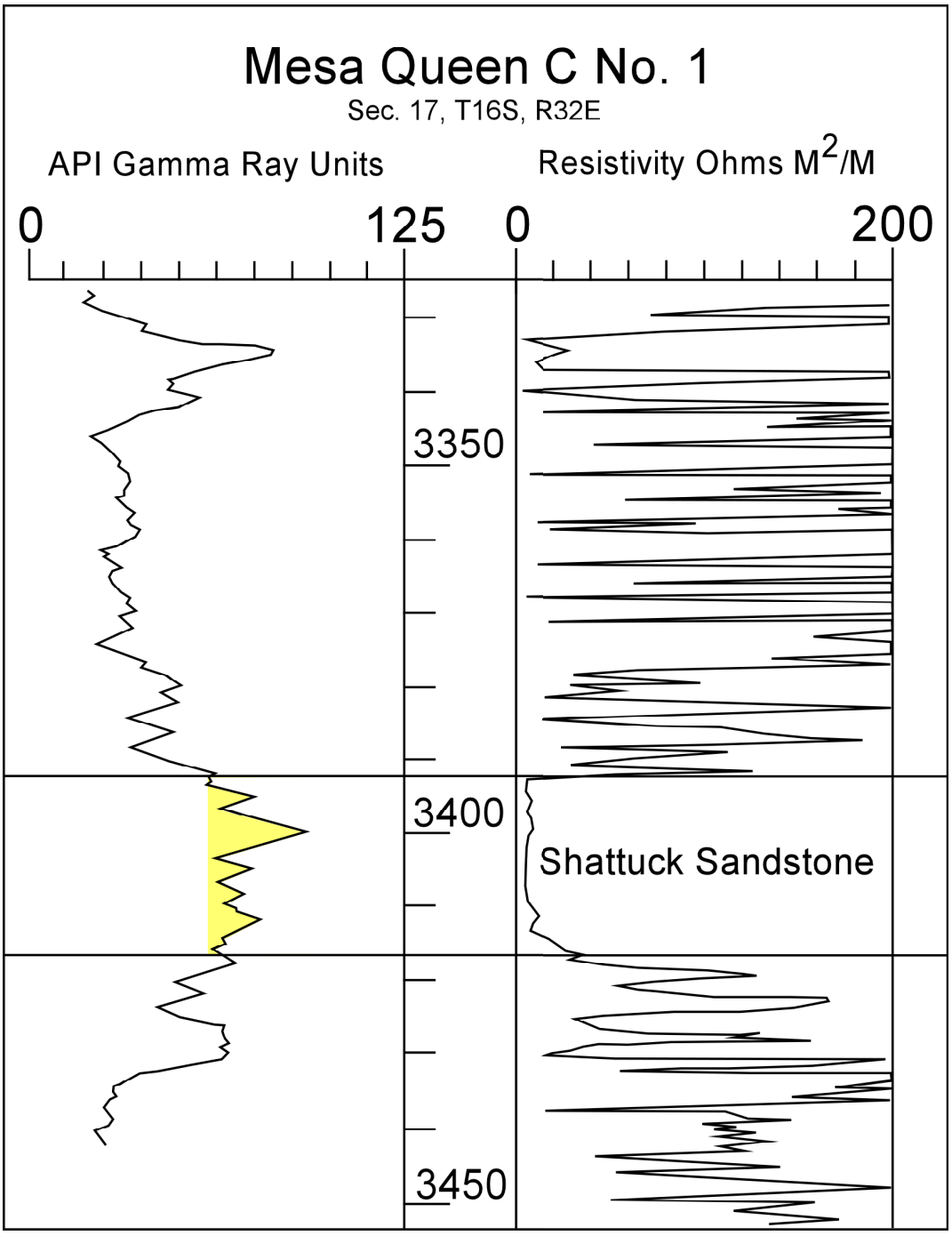

Figure 5. Typical log response (gamma ray, resistivity) from the study area showing the Shattuck Sandstone.

FIELD-SCALE PROPERTIES

Structure and Sand-Body Geometry

The top of the Shattuck Sandstone is a homocline that dips approximately 37 ft/mi (7 m/km or 0.4º dip) along the southeast regional dip (Fig. 6). The reservoir in Mesa Queen Field lacks structural closure and is interpreted to be a stratigraphic trap.

The Shattuck Sandstone is a sheet-like sand body (Fig. 7) with a local thickening. The sandstone ranges in thickness from 20 ft. (6.1 m) to 36 ft. (11.0 m), with an average thickness of 30 ft (9.1 m) within Mesa Queen Field. The sandstone has a general thickening from west to east, and the isopach map shows a local thickening that forms an elongate sand body with a northeast-southwest trend (Fig. 8). This elongate sand body contains the best producing wells within its center where the sandstone attains its maximum thickness (see appendix A for production data).

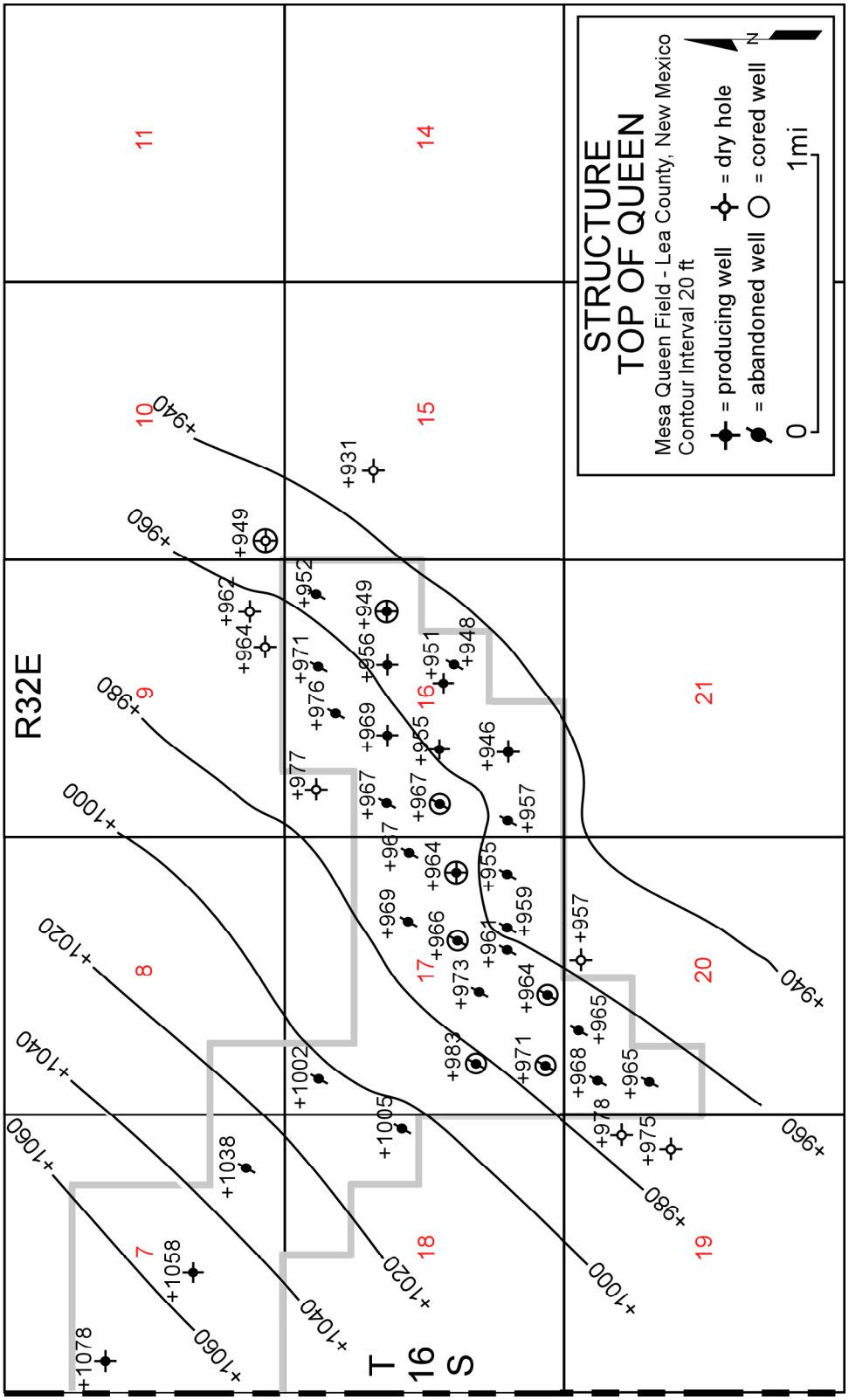

Figure 6. Structural contour map. Contours drawn on top of the top of the Queen Formation (Shattuck Sandstone) in the study area.

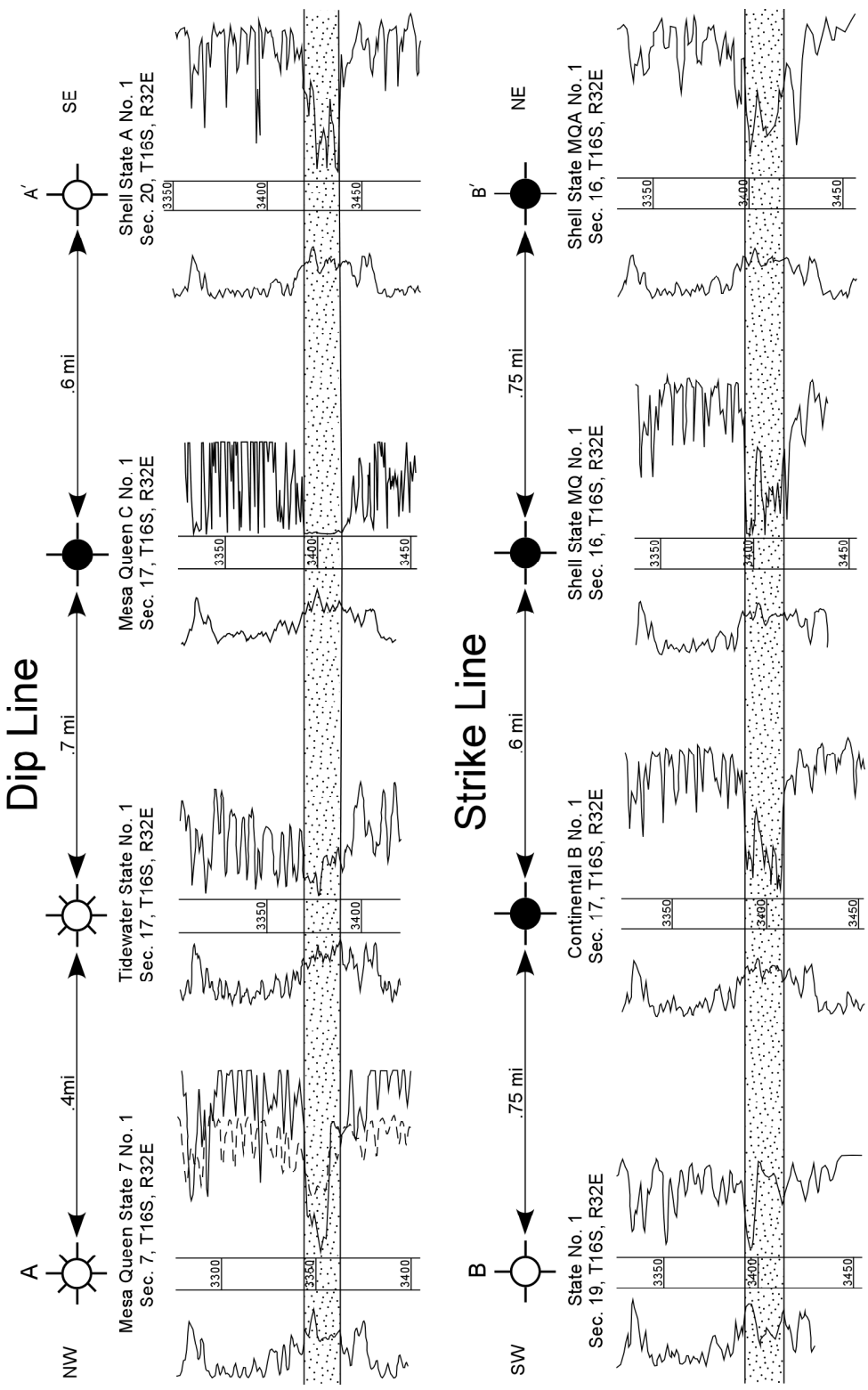

Figure 7. Dip line (A-A′) and strike line (B-B′) cross sections showing the planar geometry of the Shattuck Sandstone. Dip line shows a slight thickening in the center of the cross section.

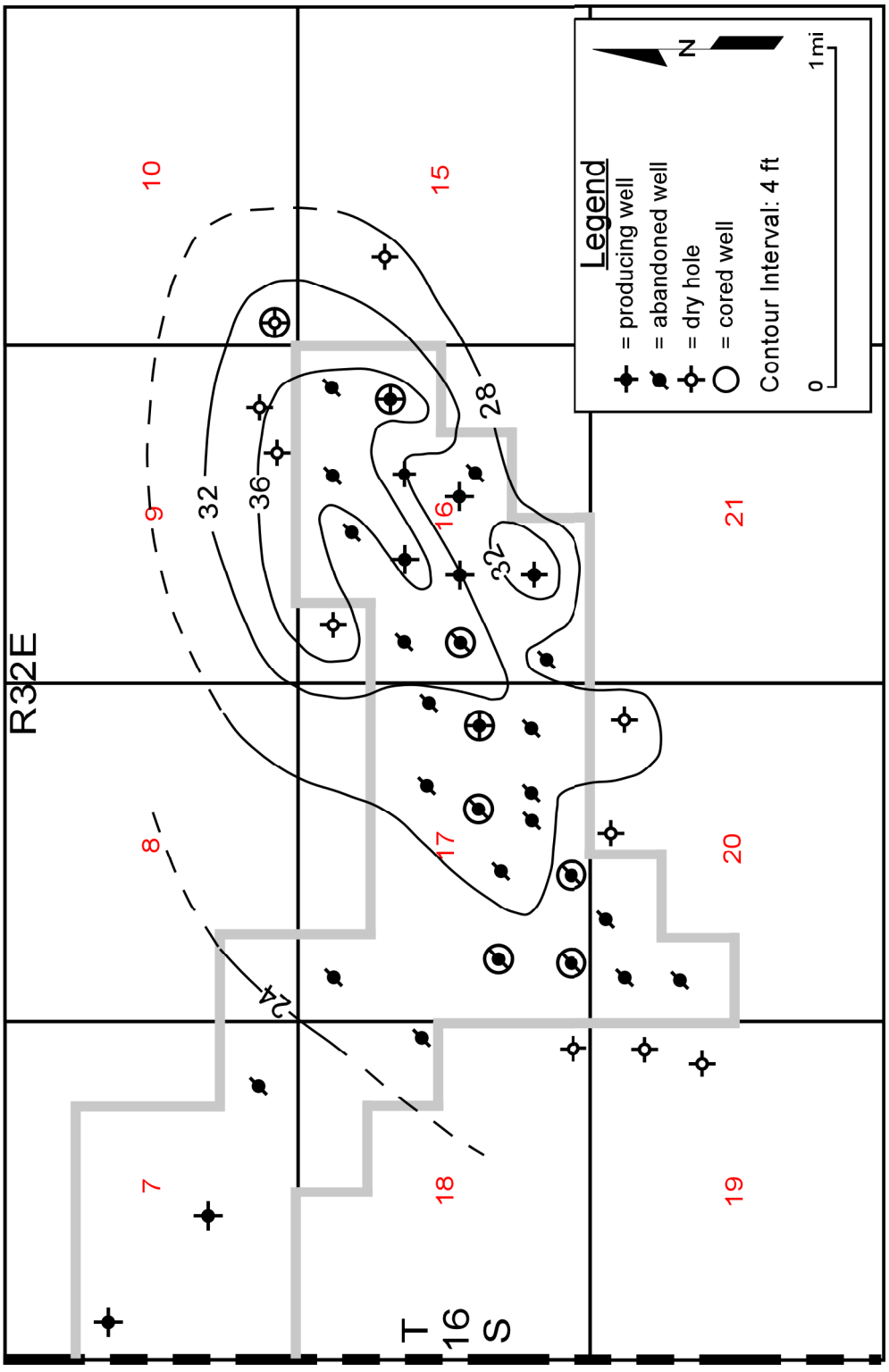

Figure 8. Isopach map of the Shattuck Sandstone showing an elongate sand body with a NE-SW trend.

FACIES AND DEPOSITIONAL ENVIRONMENTS

The Shattuck Sandstone in the study area contains four major siliciclastic facies. These facies were defined by their lithologies and sedimentary structures observed in the core; Table 1 summarizes their main characteristics.

Facies 1 Description

Facies 1 is divided into 3 distinct subfacies: Subfacies 1A, 1B, and 1C. Subfacies 1A consists of planar-, wavy-, and ripple-laminated very fine sandstones with thin mudstone drapes (Fig. 9A). It is thick- to very thick-bedded (2.7-5.7 ft; 0.82-1.73 m), and is yellowish-gray (5Y 7/2) to greenish-gray (5GY 6/1) except where oil-stained to black. Oil staining is intermittent and seems to preferentially occupy the uppermost portion of laminae. Planar and wavy laminae are both thin (<3 mm) and thick (3-10 mm). Ripple laminae are consistently thick (3-10 mm) and typically interbedded with the wavy and planar laminae. Mudstone drapes are found capping a majority of the laminae and are difficult to see in unpolished core. In thin section, thin lags of coarser quartz grains are present throughout this subfacies (Fig. 9E). The lags are usually just one grain in thickness and vary in size from medium to coarse sand.

Subfacies 1B is very fine sandstone (Fig. 9B, C, and D), which is very thick-bedded (7.1-12.1 ft; 2.15-3.70 m), has a mottled appearance, and is very friable. In many instances cores of this subfacies were composed entirely of rubble, with few pieces of consolidated rock. This subfacies varies from pale greenish-yellow (10Y 8/2) to light olive gray (5Y 6/1), except where oil-stained completely black. The mottled

Table 1. Facies, facies properties, and interpreted depositional environments.

Facies #	Lithology	Avg. Grain Size (μm)	Sedimentary Structures	Porosity (%)* High/Low/Avg	Permeability (md)** High/Low/Avg	Reservoir Potential	Depositional Environment
1A	sandstone, mudstone	90	wavy, ripples, planar	18.8 / 1.5 / 9.0	28.0 / 0.8 / 10.4	fair	fluvial sheetflood
1B	sandstone	109	wavy, cut & fill	20.8 / 3.1 / 14.0	274 / 3.9 / 50.3	very good	wadi plain
1C	sandstone, mudstone	75	chaotic, planar	13.9 / 0.5 / 8.4	1.4 / 0.1 / 2.1	poor	river mouth
2	sandstone	131	high & low angle x-beds, planar	26.9 / 0.6 / 14.0	1006 / 324 / 665	very good	eolian sand sheet
3	sandstone, siltstone, mudstone	100	chaotic, planar	19.5 / 0.0 / 4.0	<0.1 all	poor	inland sabkha
4	sandstone	115	massive, planar	30.1 / 3.9 / 15.1	804 / 6.7 / 333	very good	reworked eolian
5	dolomicrite	NA	styolitic laminations	<1.0	<0.1	poor	intertidal
6	anhydrite	NA	wavy laminations	<1.0	<0.1	poor	lagoonal
7	siltstone, mudstone	NA	wavy, planar, chaotic	<1.0	<0.1	poor	supratidal

* Porosity reported from point counts and one core analysis combined

** Permeability values obtained from core analysis from one well only.

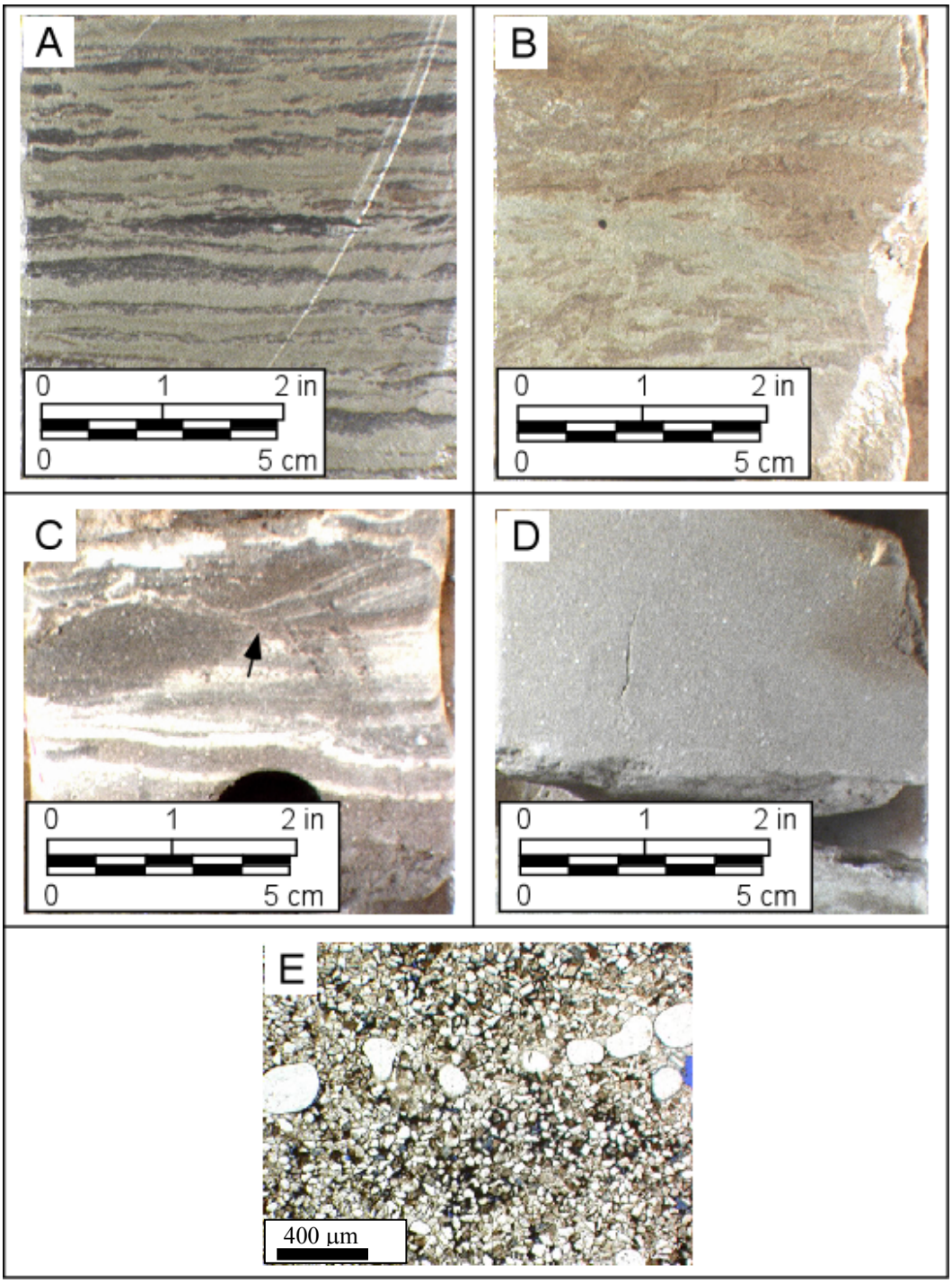

Figure 9. Core photographs of Subfacies 1A and 1B. (A) Planar, wavy, and ripple-laminated very fine sandstone of Subfacies 1A. (B) Mottled appearance of Subfacies 1B. (C) Trough cross-bedding and low-relief scour feature (arrow) of Subfacies 1B. (D) Massive very fine sandstone of Subfacies 1B. (E) Photomicrograph of Subfacies 1A showing lag deposit.

appearance is due in part to differences between oil-stained, porous and relatively unstained nonporous rock. Where mottling does not obscure primary sedimentary structures, wavy beds and trough cross-beds underlain by low-relief scour features were observed (Fig. 9C). The low-relief scour structures are rare in abundance, but are distinctive features of this subfacies. Medium-bedded (0.5-1.0 ft; 0.15-0.30 m) massive sandstones (Fig. 9D) are also found at irregular intervals within this subfacies.

Subfacies 1C is very fine sandstone and silty mudstone that is thick- to very thick-bedded (1.0-4.0 ft; 0.3-1.2 m). It generally varies from pale olive (10Y 6/2) to dark greenish-gray (5GY 4/1), but rarely is dark reddish-brown (10R 3/4; Fig. 10A). Chaotic bedding is common, but thin (<3 mm), planar and wavy laminae were observed (Fig. 10B). This subfacies is always found overlying the wadi deposits of Subfacies 1B.

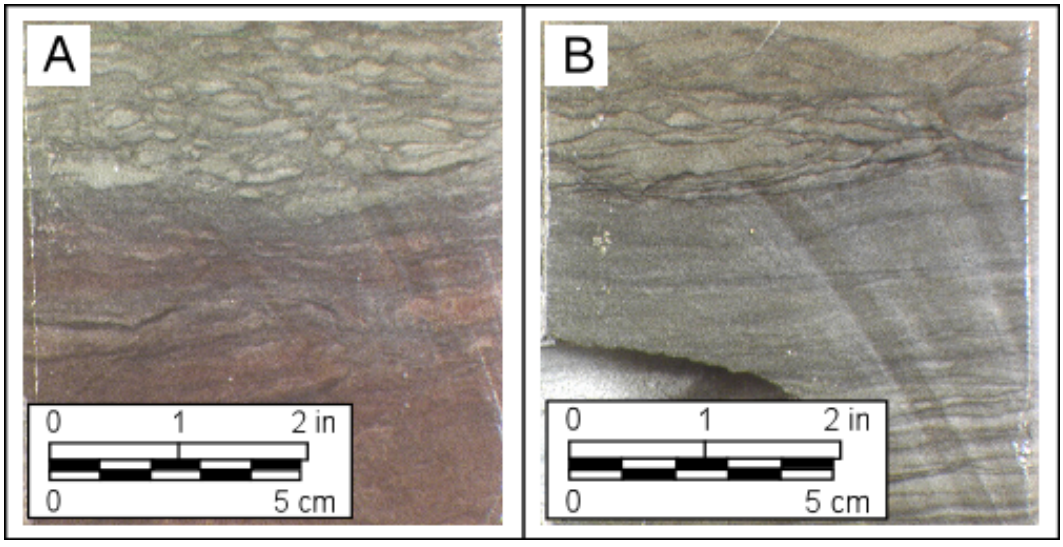

Figure 10. Core photographs of Subfacies 1C. (A) Chaotic bedding of Subfacies 1C. (B) Planar laminae of Subfacies 1C bounded above and below by chaotic bedding.

Facies 1 Interpretation

Facies 1 was deposited on gently sloping fluvial sandflats at the downslope end of alluvial fans. Braided streams, common to proximal parts of alluvial fans, expand as slopes decrease until flows pass into sheet floods over fluvial sandflats (Hardie et al., 1978). Wadis (small, steep-walled, erosional channels) commonly cut locally into sandflats in desert settings. Wadis are only active during major desert storms when heavy rainfall produces flash floods across wide areas of the sandflat. Because the flow of water in wadis is sporadic and not well maintained, channel avulsion is common (Glennie, 1970).

Subfacies 1A is fluvial sandflat sheetflood deposits. During storms, water can break through channel banks and spread out as a broad unconfined sheet. The resulting deposits are commonly horizontally laminated sands. In a modern study of wadi flood deposits (McKee et al., 1967), it was estimated that 90-95% of the sediments deposited from a recent flood contained horizontal laminae. In the remainder, sedimentary structures included tabular cross bedding, climbing ripple stratification, and convolute bedding. Lag deposits seen in thin section are wind deflation surfaces formed on fluvial sandflats between major storm depositional events.

Subfacies 1B is deposits of channels (wadis) crossing the fluvial sandflat. Low-relief scours and overlying lag deposits formed during storm runoff events that caused incision of the fluvial sandflat. As the flow of water decreased, channels were filled with sands containing wavy and trough cross-bedding, and massive beds.

Subfacies 1C is the sediments deposited at the mouth of the wadi. Abundant

mud laminations and fine grain size indicate a low energy environment and waning flow able to releases fines from suspension. Most of the primary sedimentary structures were destroyed after deposition due to haloturbation and sabkha-like processes (e.g., repetitive formation and dissolution of soluble evaporative minerals). This subfacies is always found overlying the wadi deposits of Subfacies 1B.

Facies 2 Description

Facies 2 is fine to very fine sandstone with sedimentary structures that include cross-beds, planar laminae, planar-inclined laminae, and massive beds (Fig. 11). These sandstones are interbedded in medium to very thick bedsets (1.0-14.7 ft; 0.6-4.5 m), and are usually oil-stained to a yellowish-gray (5Y 7/2) or black color. Where oil staining is not present, as is the case for one dry hole on the northeastern boundary of the field area, these sandstones tend to be a dark reddish-brown (10R 3/4) to moderate reddish-brown (10R 4/6) color. The cross-beds are 0.3-1.5 ft (0.10 to 0.46 m) thick and contain high-angle (15-25º) foresets (Fig. 11A and C). These foresets are composed of thin (< 3 mm), planar cross-laminae with rare wedge-planar laminae. The planar-laminated beds are 0.3-1.1 ft (0.10 to 0.35 m) thick and are composed of thin (< 3 mm) laminae (Fig. 11B). The planar-inclined laminations are found in beds ranging from 0.3-1.0 ft (0.1 to 0.4 m) in thickness (Fig. 11D), and have dips less than 15º relative to cross-set boundaries. Massive beds are 0.1 to 0.3 m thick. Also common to this facies is unusually large quartz grain lags (similar to those seen in Subfacies 1A). The large quartz grains tend to be more scattered in this facies, and lags were never seen in close proximity to one another like those found in Subfacies 1A.

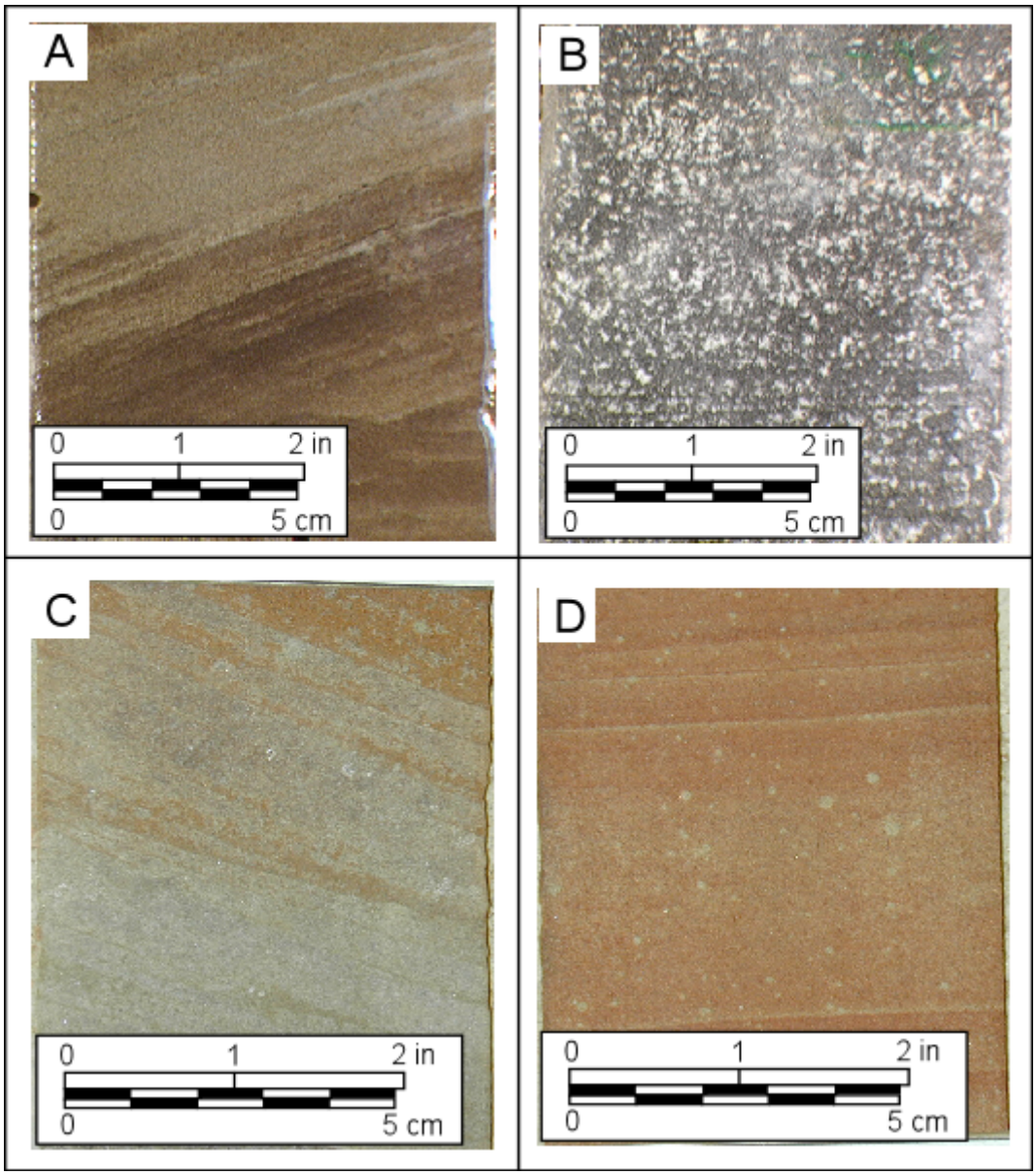

Figure 11. Core photographs of Facies 2. (A) High-angle cross-beds (B) Oil-stained appearance of Facies 2, massive at top with faint planar laminae near bottom. (C) High-angle cross-beds with wedge-shaped foresets. (D) Planar-inclined laminae.

Facies 2 Interpretation

Facies 2 is deposits of eolian sand sheets. Eolian sand sheets are low-lying sand deposits that result from either deposition or erosion. They vary greatly in both size and morphology. Sand sheets can occupy small interdune areas or be of great areal extent. A modern sand sheet at Great Sand Dunes National Monument, Colorado covers 274 mi^2 (710 km^2; Fryberger et al., 1979). Wind-ripple laminae with horizontal to low-angle (<20º) dip (Ahlbrandt and Fryberger, 1982; Kocurek and Nielson, 1986), and less common isolated dunes, occur on sand sheets.

Horizontal and low-angle laminae within Facies 2 are the wind-ripple laminae indicative of eolian sand sheets. High-angle cross-bed laminae are foresets of small dunes that periodically formed when long spells of aridity made loose sand readily available. Wedge-shaped foresets likely record the slumping or avalanching of sand deposited at dune slip face toes. Such avalanche toes are common at the base of sand dunes, and have been described in both modern and ancient eolian dune environments (Hunter, 1977; Kocurek and Dott, 1981; Ahlbrandt and Fryberger, 1982; Fryberger et al., 1983).

Facies 3 Description

Facies 3 is deformed, wavy and planar-laminated very fine sandstone to siltstone beds with silty mudstone drapes and displacive nodular anhydrite (Fig. 12). These lithologies are interbedded in very thick bedsets (6.5-14.8 ft; 2.0 to 4.5 m). This facies is commonly dark reddish-brown (10R 3/4), and in places, dark gray (N3). Beds deformed within this facies are generally 0.25-2.0 ft thick (0.07-0.6 m). Mudstone drapes are both

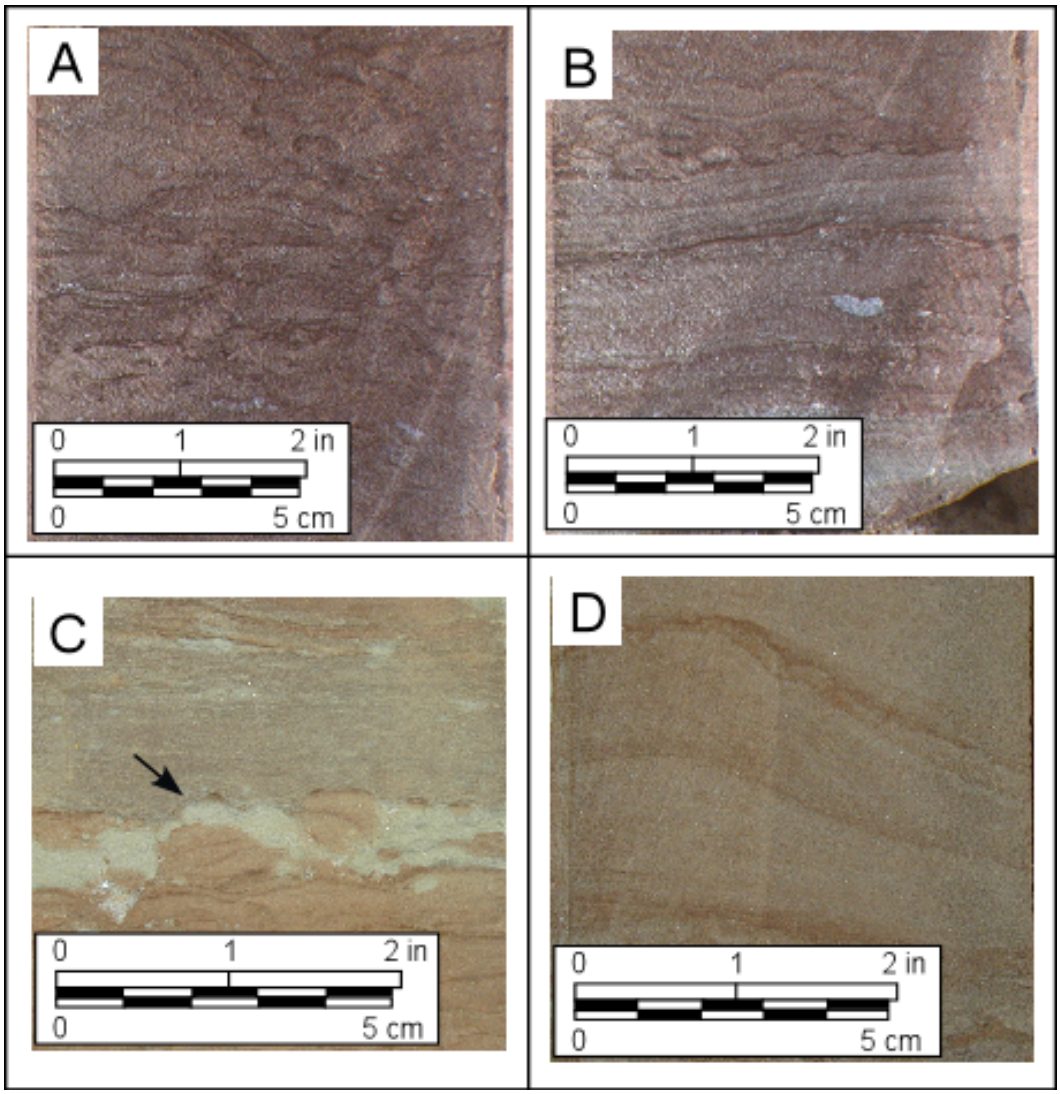

Figure 12. Core photographs of Facies 3. (A) Disruptive and chaotic bedding. (B) Both chaotic and planar to wavy bedding (note nodular anhydrite). (C) Knobbly surface (arrow) overlain by laminated sandstones and siltstones. (D) Boudinage-like feature that could be a salt ridge structure.

continuous and discontinuous parallel laminae that range in color from dark reddish-brown (10R 3/4) to dark gray (N3). Discontinuous mudstone drapes are more common where the bedding has been highly deformed and are in the form of nonparallel laminae. In one instance, a knobbly or disturbed bedding surface was seen (Fig. 12C). Other deformation features present include microfaults, fluid escape structures, and boudinage-like structures that thicken and thin. The microfaults and fluid escape structures are very small and rare.

Planar-laminated beds occur within very thin to thin (0.06-0.13 ft; 0.06-0.13 m) beds, and are composed of alternating layers of siltstones and mudstone drapes. Mudstone drapes occur both as wavy and planar parallel laminae. The nodular anhydrite varies from white to light bluish-gray (5B 7/1). Individual nodules vary in size from 1 mm to 1 cm in diameter, and are either circular to ovate in shape. Nodular-mosaic anhydrite is also present, but is much more rare than individual anhydrite nodules.

Facies 3 Interpretation

Facies 3 is deposits of inland sabkhas. Inland sabkhas are flat, low-lying sand or mud flats that receive siliciclastic sediment by fluvial, eolian, and suspension settling processes. They are characterized by evaporite crusts that form on or near their surface due to evaporation of groundwater and surface water. Brief, torrential storms lead to flooding of sabkhas as sheetfloods spread across the sabkha surface. These storms may be seasonal or many years apart (Glennie, 1970; Lowenstein and Hardie, 1985; Warren, 1989). Aridity following storm events desiccates the sabkha, and evaporites precipitate at or near the surface. Expansive growth of evaporites causes the sabkha surface to

buckle and warp, destroying depositional sedimentary structures recently formed. As desiccation becomes more prolonged, eolian processes dominate leading to the formation of eolian sand sheets. During a subsequent storm, renewed influx of fresh meteoric water will dissolve soluble evaporite minerals (e.g. halite), leading to further disruption of sediments.

Planar and wavy laminations are deposited by upper flow regime sheetfloods during storms. Mudstone drapes are deposited as the fines settle from suspension following sheetfloods.

The expansive growth of nodular anhydrite (haloturbation) disrupted the inland sabkha sediments. Nodular anhydrite was presumably precipitated just below the surface, near and in the capillary zone during periods of aridity as in modern sabkhas. Sabkhas of the Trucial Coast have been studied extensively, and it has been found that modern-day anhydrite is forming in the capillary zone just above the water table there. Below the water table, however, the anhydrite is no longer stable and is hydrated to gypsum (Kinsman, 1969; Fryberger et al., 1983; Warren and Kendall, 1985; Warren, 1989). Whether anhydrite originally precipitated as gypsum is unclear, as distinct crystal morphology suggesting anhydrite psuedomorphs after gypsum were not observed. The disturbed appearance of Facies 3, and the formation of other deformation features such as microfaults, can be partly attributed to the displacive growth of nodular anhydrite. Chaotic and disruptive bedding, however, is present even in the absence of nodular anhydrite. This suggests that a more soluble mineral phase was initially precipitated, then later dissolved during subsequent flood events.

Boudinage-like features are interpreted to be salt-ridge structures formed at or near the surface due to evaporation of saline capillary water. Expansive evaporite growth causes the salt layer surface to rise (Fryberger et al., 1983). Although different in appearance, the knobbly or puffy surfaces (Fig. 12C) formed in the same manner, and record continual deposition and disruption of a growing salt layer (Warren, 1989).

Fluid escape structures form by water escaping through liquefied sediments (Lowe, 1975). It is likely that periodic flooding of the sabkha surface from storms led to the liquefaction of near-surface sediments, and resulted in the formation of fluid escape structures.

Facies 4 Description

Facies 4 is fine to very fine sandstone with very thin silty mudstone interlaminations (Fig. 13). Thick- to very thick-bedded (3.0-7.0 ft; 0.91-2.13 m), it has a relatively clean appearance reflecting little matrix mud. Sandstones of this facies are yellowish-gray (5Y 7/2) to greenish-gray (5GY 6/1), and mudstone laminations are dark greenish-gray (5GY 4/1). Nodular anhydrite is present, but rare. Sedimentary structures include both wavy and planar beds often separated by the silty mudstone laminations. Where these laminations are absent, this facies is massive to homogenized in appearance with no apparent sedimentary structures. This facies clearly fines upward into a muddy, fine to very fine sandstone. The muddier portion of this facies consistently occurs within the uppermost portion of the facies and averages 0.5 ft (0.15 m) in thickness. This portion of Facies 4 is dominated by discontinuous, wavy laminations (Fig. 13C).

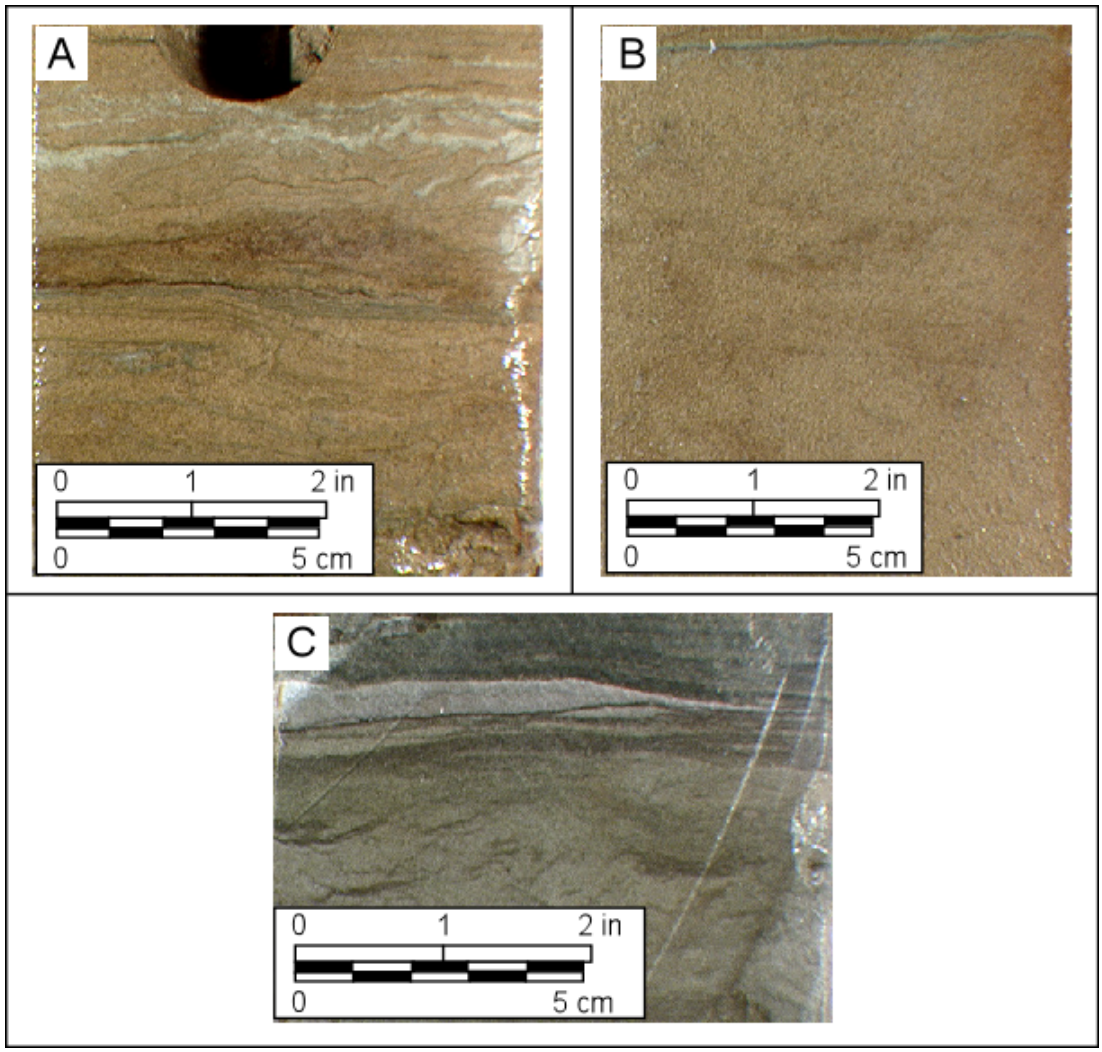

Figure 13. Core photographs of Facies 4. (A) Wavy laminations, possibly algal in origin, of Facies 4. (B) Massive appearance of Facies 4 with thin lamination at top. (C) Muddier appearance of Facies 4. Lighter, tongue-shaped portion near top is silty dolomicrite and marks the top of the Shattuck Sandstone.

Facies 4 Interpretation

Facies 4 was deposited during transgressive marine reworking of eolian and possibly fluvial sandflat deposits in nearshore environments. Although similar to Facies 2 and Subfacies 1B in grain size, it lacks evidence of wind-laid deposition. The silty mudstone laminations indicate deposition was partly influenced by water. However, sedimentary structures indicating wadi deposition (i.e., low-relief scour features and trough cross-bedding) are absent. Facies 4 is found only in the upper portion of the Shattuck Sandstone, directly below the silty dolomicrite of Facies 5.

Marine reworking of eolian sands in similar depositional settings is found elsewhere in the rock record and has been reported by other workers (Fryberger, 1986; Reese, 1984; Chan and Kocurek, 1988). Fryberger (1986) noted that marine reworking usually manifests itself as water-laid deposits composed of sand similar to the underlying dunes, or as contorted stratification below an erosion surface. Although contorted stratification was not seen in Facies 4, homogenized sand was. Also, Facies 4 is always found at the very top of the Shattuck Sandstone, directly below the silty dolomicrite of Facies 5. The contact between the two is sharp, and very likely erosional in nature.

Bounding Facies

The Shattuck Sandstone is bounded by the overlying Seven Rivers Formation and below by other facies within the Queen Formation. These bounding facies are carbonates, evaporites, siltstones, sandstones, and mudstones. From these lithologies and their internal sedimentary structures, three facies can be identified in the rocks

immediately bounding the Shattuck Sandstone.

Facies 5 Description

Facies 5 is silty dolomicrite. This facies is seen directly overlying the Shattuck Sandstone in all of the cores of the field area. The silty dolomicrite can be either thin laminations (Fig. 14B) within anhydrite or a single bed (Fig. 14F and G) that is thin-to thick-bedded (0.5-1.2 ft; 0.15-0.36 m). The single bed of silty dolomicrite contains thin (< 3 mm) laminae that contain dark gray styolitic laminae of carbonaceous silty mudstone that is possibly algal in origin (Mazzullo, 1991). It is yellowish-gray (5Y 8/1) and has small anhydrite-filled fenestrae (bird's eye) structures. In some cases, this facies is seen with a single moderate red (5R 4/6) silty mudstone lamination capping an irregular surface (Fig. 14F).

Facies 5 Interpretation

Thicker beds of Facies 5 are deposits of lower supratidal to intertidal environments seaward of a coastal sabkha. Laminated dolomicrites within bedded and laminated anhydrite, however, is deposits of an evaporative lagoon. In modern sabkha environments, dolomite is found deposited as a lagoonal mud, and as a crust in both the intertidal and supratidal zones. Dolomite found in Abu Dhabi sabkha of the Trucial Coast is neither detrital nor primary, it is diagenetic (Warren, 1991). The dolomite there is found beneath sabkha sediments and is found partially replacing aragonitic muds. In the nearby coastal sabkhas of Qatar, the dolomite is found underlying intertidal facies and is also replacing aragonitic muds there (Warren, 1991). Another line of evidence for this interpretation lies in the features of Facies 5. Algal mats are typically found in

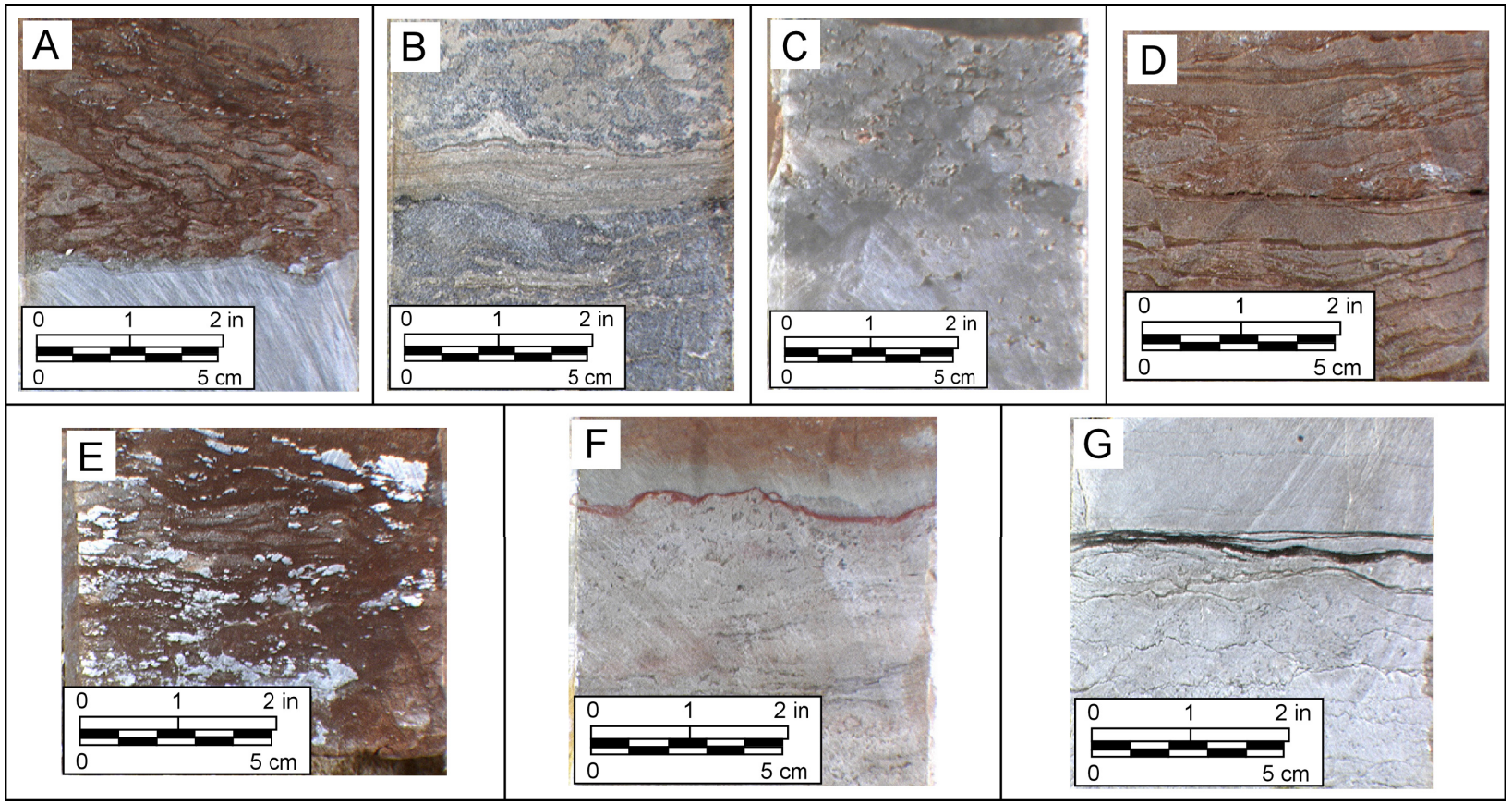

Figure 14. Core photographs of Facies 5, 6, and 7. (A) Bedded anhydrite of Facies 6 overlain by very fine sandstones and silty mudstones of Facies 7. (B) Bedded anhydrite of Facies 6 with laminated and interspersed dolomicrite of Facies 5. (C) Massive-bedded anhydrite of Facies 6. (D) Very fine sandstone with silty mudstone drapes of Facies 7. Note the disturbed bedding and mud cracks. (E) Abundant nodular and nodular-mosaic anhydrite within Facies 7. (F) Silty dolomicrite of Facies 5 capped with a single red mud lamination and overlain by the anhydrite of Facies 6. (G) Silty dolomicrite of Facies 5 with styolitic features separated by black, possible, algal laminations.

environments which receive periodic exposure such as intertidal and supratidal environments. The thin and dark laminations found in this facies are likely algal in origin. The presence of styolitic laminations and fenestral voids also indicates this environment was characterized by periodic exposure. According to Shinn (1983), fenestral structures are considered reliable indicators of intertidal to supratidal deposition.

Facies 6 Description

Facies 6 is medium-to thick-bedded (0.5-3.0 ft; 0.15-0.92 m) anhydrite (Fig. 14A, B, and C). The anhydrite varies from laminated to massive, is commonly a light to medium bluish-gray (5B 7/1-5B 5/1), and contains rare pyrite nodules. Both dolomicrite and dark reddish-brown (10R 3/4) silty mudstone laminae are found capping irregular surfaces within the anhydrite and filling rare vertical fractures.

Facies 6 Interpretation

Facies 6 is the deposits of an evaporative lagoon. This anhydrite was precipitated from hypersaline lagoonal waters during long periods of aridity, and/or during periods of poor water circulation in the back-reef environments. The great thickness of the anhydrite beds is evidence the anhydrite formed in a standing body of water. The irregular surfaces capped with dolomicrite and silty mudstone laminae are dissolution surfaces. These dissolution surfaces could have formed as a result of (1) periodic exposure of the lagoonal sediments during sea-level fluctuations, or (2) a drop in salinity of the lagoonal waters, either by increased circulation with normal marine waters or by an increased influx of meteoric waters.

Facies 7 Description

Facies 7 is very fine sandstones, siltstones, and silty mudstones interbedded with abundant nodular and nodular-mosaic anhydrite, and the bedded anhydrite of Facies 6 (Fig. 14A, D, and E). The sandstones and mudstones are dark reddish-brown (10R 3/4), whereas the anhydrite is light to medium bluish-gray (5B 7/1-5B 5/1). Deformed bedding is very abundant, but sedimentary structures such as mud cracks, and wavy to planar silty mudstone laminae were observed (Fig. 14D).

Facies 7 Interpretation

Facies 7 was deposited in the supratidal zone of a coastal sabkha. The anhydrite present is common to supratidal sediments of arid settings, both modern and ancient. Anhydrite in this facies formed in the capillary zone in a similar manner to that interpreted for Facies 3 (inland sabkha). However, Facies 7 contains a greater abundance of anhydrite than does Facies 3, which may reflect differences in the nature of groundwater replenishment. Groundwater underlying inland sabkhas is mainly derived from continental groundwater replenished by meteoric water, whereas that underlying coastal sabkhas gets replenished by marine waters during high tides, storm flooding, and possibly by the lateral flow of seawater (Kinsman, 1969). The presence of mud cracks in Facies 7 indicates periodic wetting and desiccation phases, which are typical of coastal sabkhas.

Facies Successions

Two facies successions were observed in the Shattuck Sandstone (Figs. 15, 16, and 17). The MQ #1 well (Fig. 16A) completely penetrates the Shattuck Sandstone, while

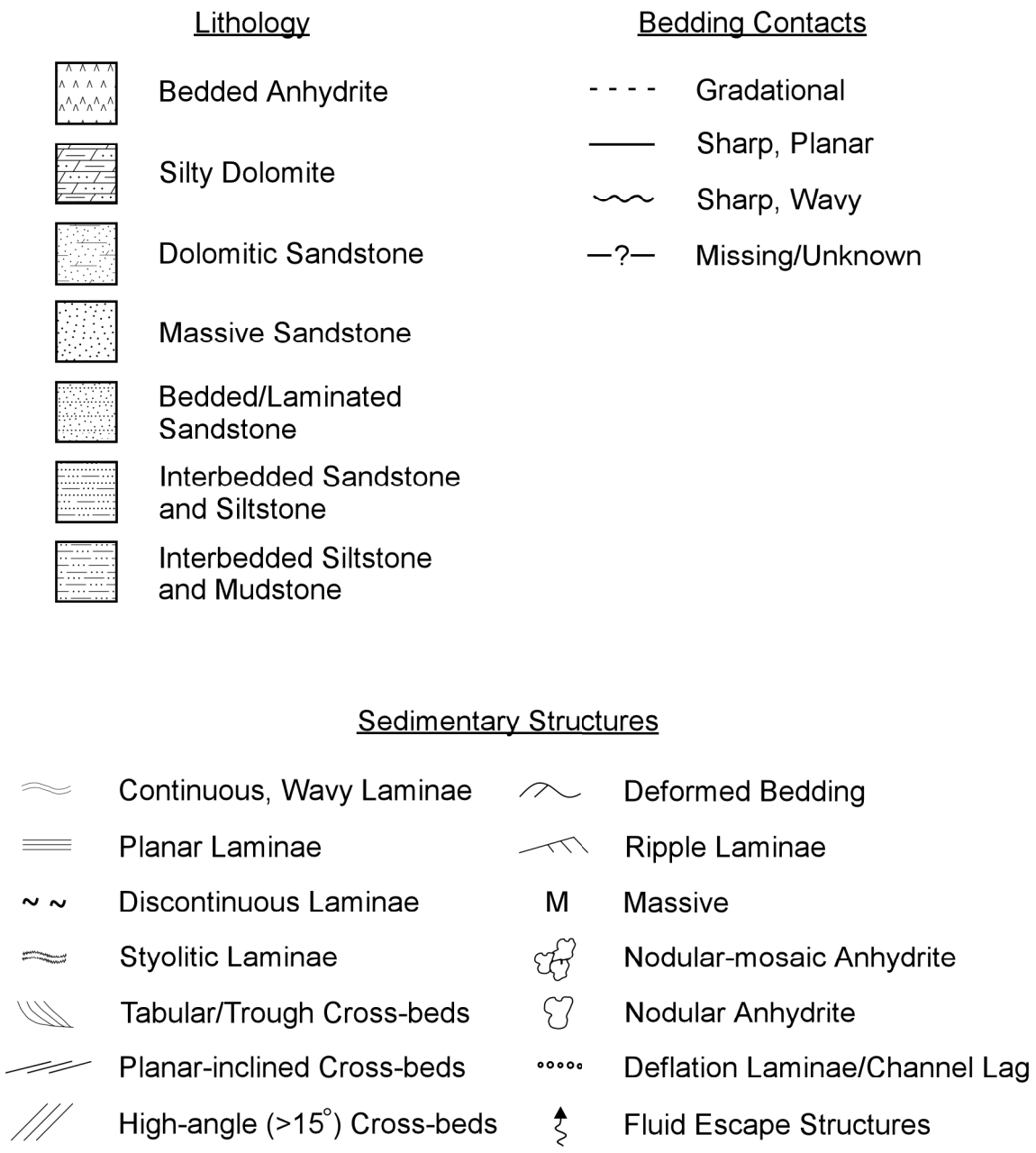

Figure 15. Legend for lithostratigraphic columns.

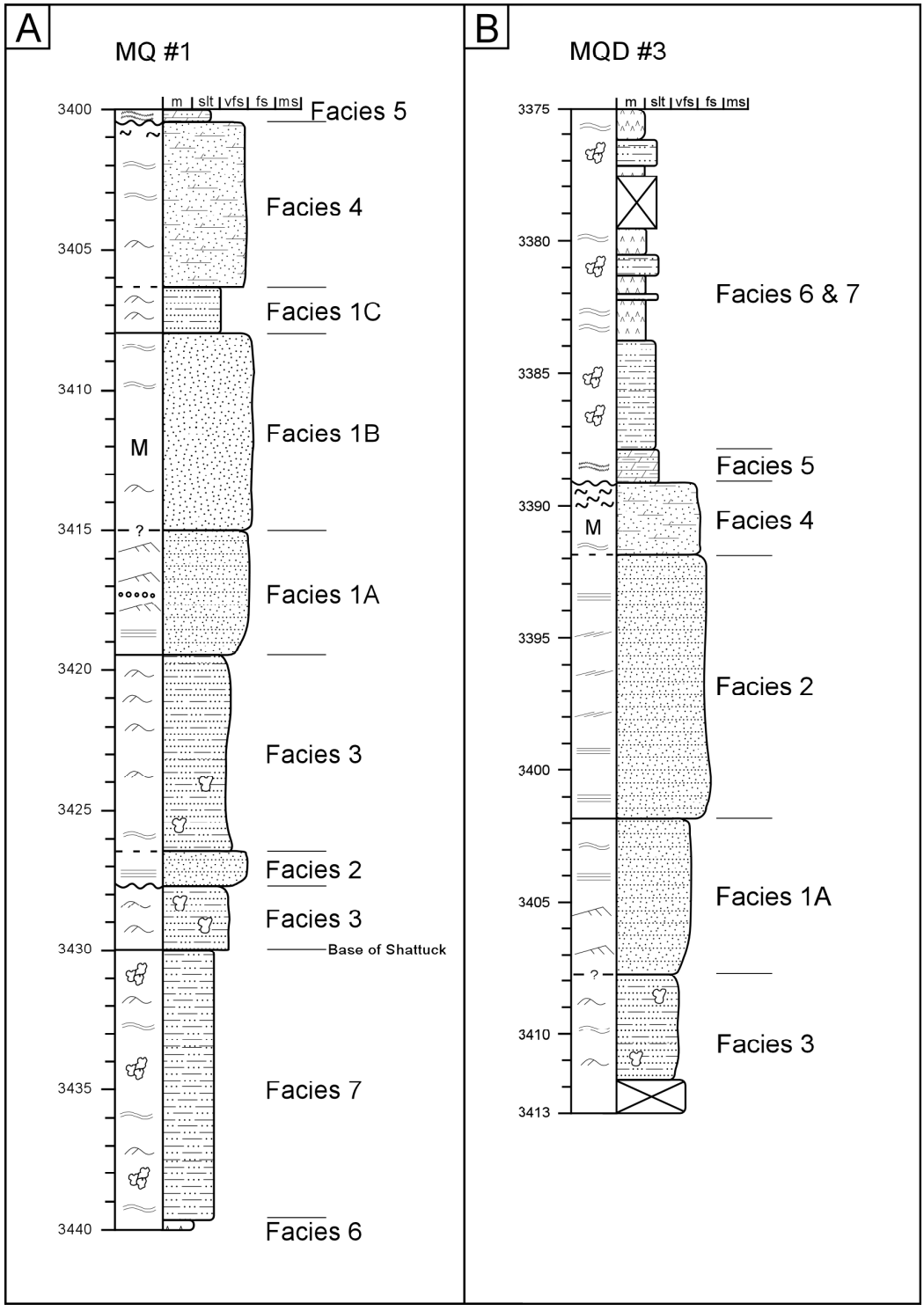

Figure 16. Typical stratigraphic successions of the Shattuck Sandstone. (A) Litho-stratigraphic log for the MQ #1 well. (B) Lithostratigraphic log for the MQD #3 well.

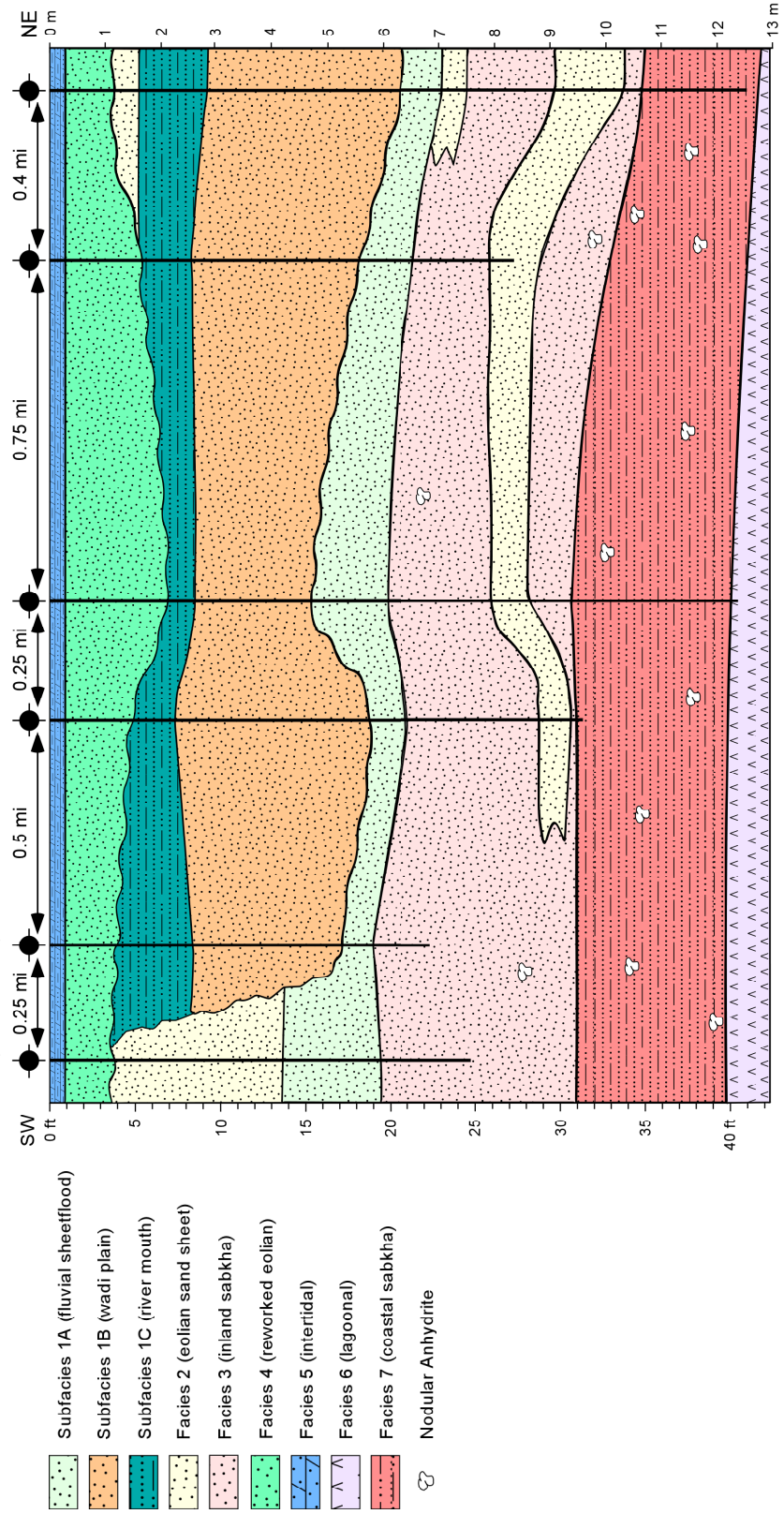

Figure 17. SW-NE (strike) cross-section showing stratigraphic nature of facies and depositional environments. Note: vertical exaggeration is approximately 210

the MQD #3 well (Fig. 16B) does not. Therefore, the MQ #1 well shows Facies 6 and Facies 7 bounding the Shattuck Sandstone from below. The basal contact of the Shattuck Sandstone is sharp, planar, and likely erosional. Facies 3 occurs at the base of the Shattuck Sandstone and contains a thin interval of Facies 2. Facies 3 is directly overlain by Subfacies 1A across the study area, and the contact between the two is sharp and planar. Facies 1B unconformably overlies Subfacies 1A over most of the study area. Where Subfacies 1B is absent, a thick interval of Facies 2 is found. This is the main difference in the stratigraphic succession across the study area, and this facies change occurs over a very short lateral distance.

The next major difference in stratigraphic successions is the presence of Subfacies 1C. Subfacies 1C gradationally overlies Subfacies 1B only. Facies 4 gradationally caps the top of the Shattuck Sandstone over the entire study area. The top of the Shattuck Sandstone is marked by a single bed of silty dolomicrite (Facies 5). This contact is always sharp.

Interpretation of Facies Successions

Deposition of the Shattuck Sandstone was initiated by a fall in sea level, which led to progradation of siliciclastics across the Northwest Shelf. During the initial stages of deposition, the study area was occupied by an inland sabkha that deposited sediments over the adjacent coastal sabkha. Periods of prolonged aridity desiccated inland sabkha sediments and led to the formation of sporadic, small eolian sand sheets. As progradation continued, fluvial sandflats formed by sheetflood processes. Increased sediment flux was later supported by the initiation of wadi systems. Eolian sand sheets

also formed during arid periods in these environments, but they were possibly larger than their inland sabkha predecessors as more sediment became available for entrainment by wind. During later stages of deposition of the Shattuck Sandstone, the eolian and wadi sediments were reworked during marine transgression. Coastal sabkha and lagoonal deposits at the top of the Shattuck Sandstone reflect this sea-level rise. Figure 18 is a depositional model that illustrates the likely distribution of environments present during the deposition of the Shattuck Sandstone.

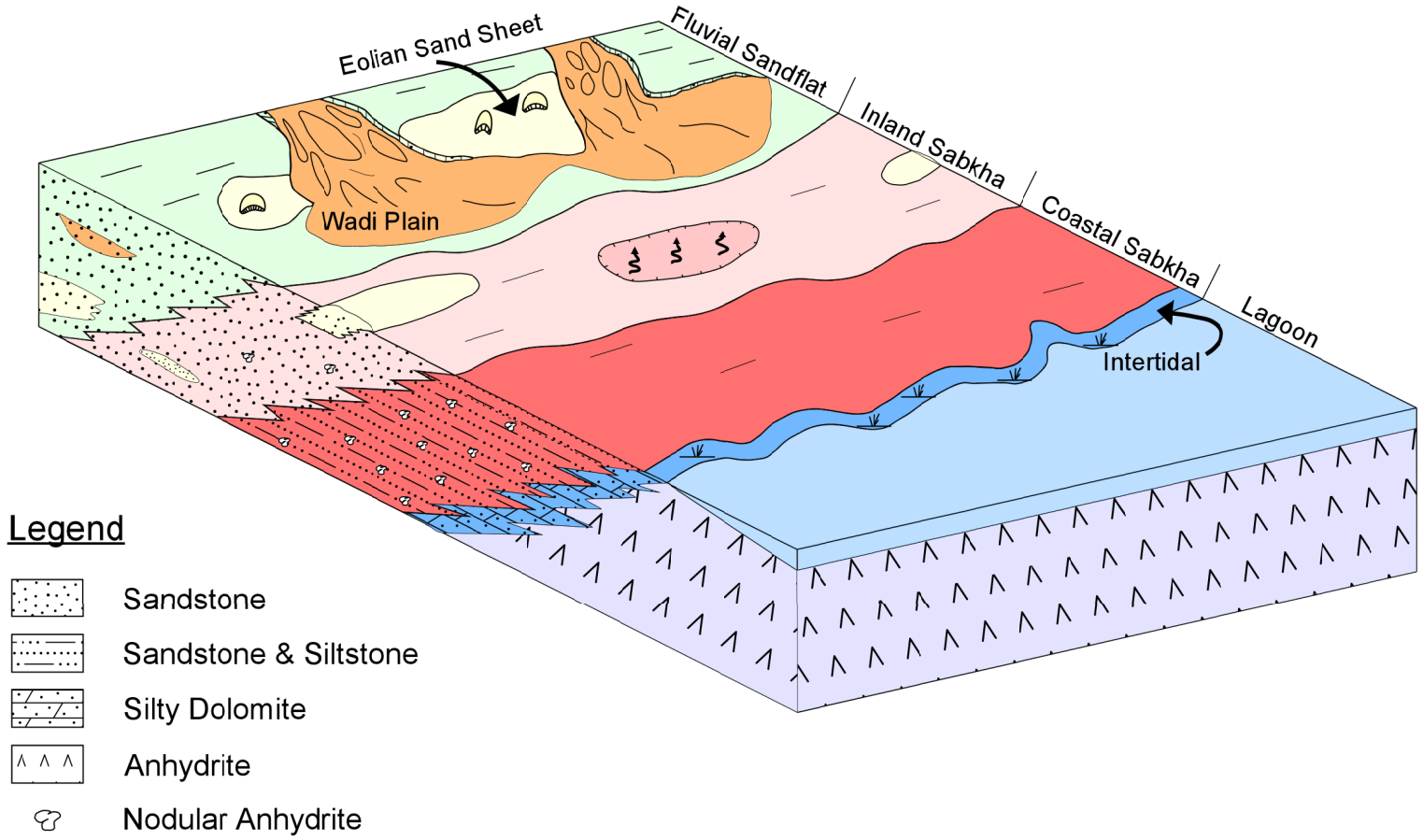

Figure 18. Depositional model of the Shattuck Sandstone. Note that model is not to scale.

GRAIN PROPERTIES

Grain properties of the Shattuck Sandstone include grain size, composition, and diagenetic history. This section examines the Shattuck Sandstone in order to classify it in terms of composition. Textural features are examined to better characterize the facies and relate their features to depositional and diagenetic processes.

Grain Size

The Shattuck Sandstone at Mesa Queen Field is predominantly a moderately- to well-sorted, very fine-grained sandstone with minor amounts of siltstone and mudstone. The average grain size for all samples of the sandstone is 98 microns (3.55ϕ), which is equivalent to very fine-grained sand. Mean sizes range from 59 to 135 microns (4.08ϕ to 2.89ϕ), and individual grains range in size from 16 to 854 microns (5.97ϕ to 0.23ϕ). The mean standard deviation (i.e., sorting, σ) of all samples is 42 microns (0.6ϕ), and standard deviations of individual samples range from 22 to 78 microns (0.44ϕ to 0.67ϕ). A mean standard deviation of 42 microns corresponds to 0.6ϕ, and in verbal terms is moderately well sorted (Folk, 1974).

Grain size distributions for each environment are shown as histograms and cumulative frequency curves (Figs. 19 and 20). Mean grain sizes and standard deviations for the different facies are similar. The coarsest samples are from the eolian sand sheet facies (Fig. 20), which have a mean grain size of 117 microns (3.1ϕ). Eolian environments are dominated by wind energy and tend to be coarser due to the winnowing of fine sediments by the wind. Conversely, the river-mouth facies (with a

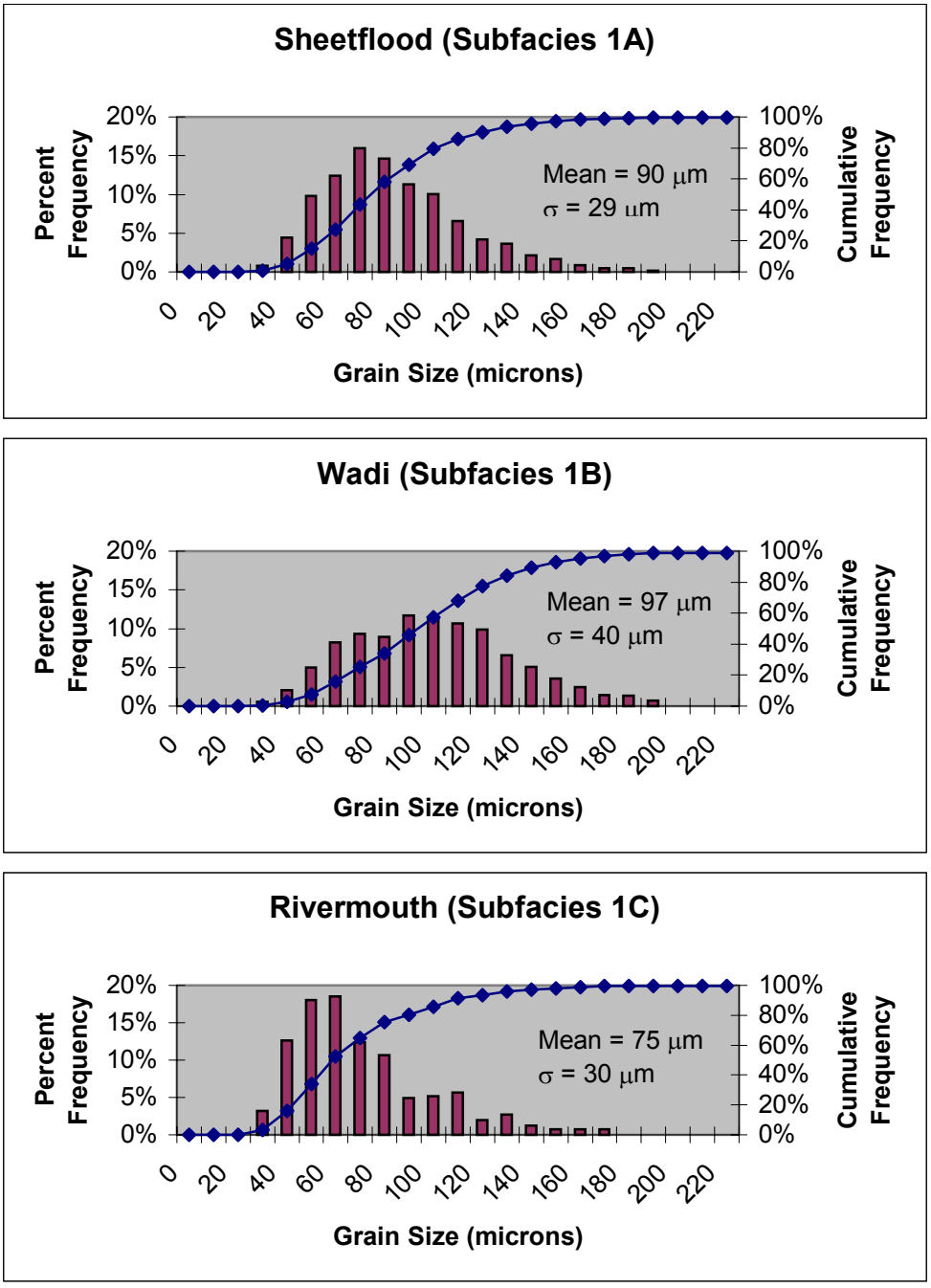

Figure 19. Frequency distributions for sheetflood, wadi, and river mouth depositional environments.

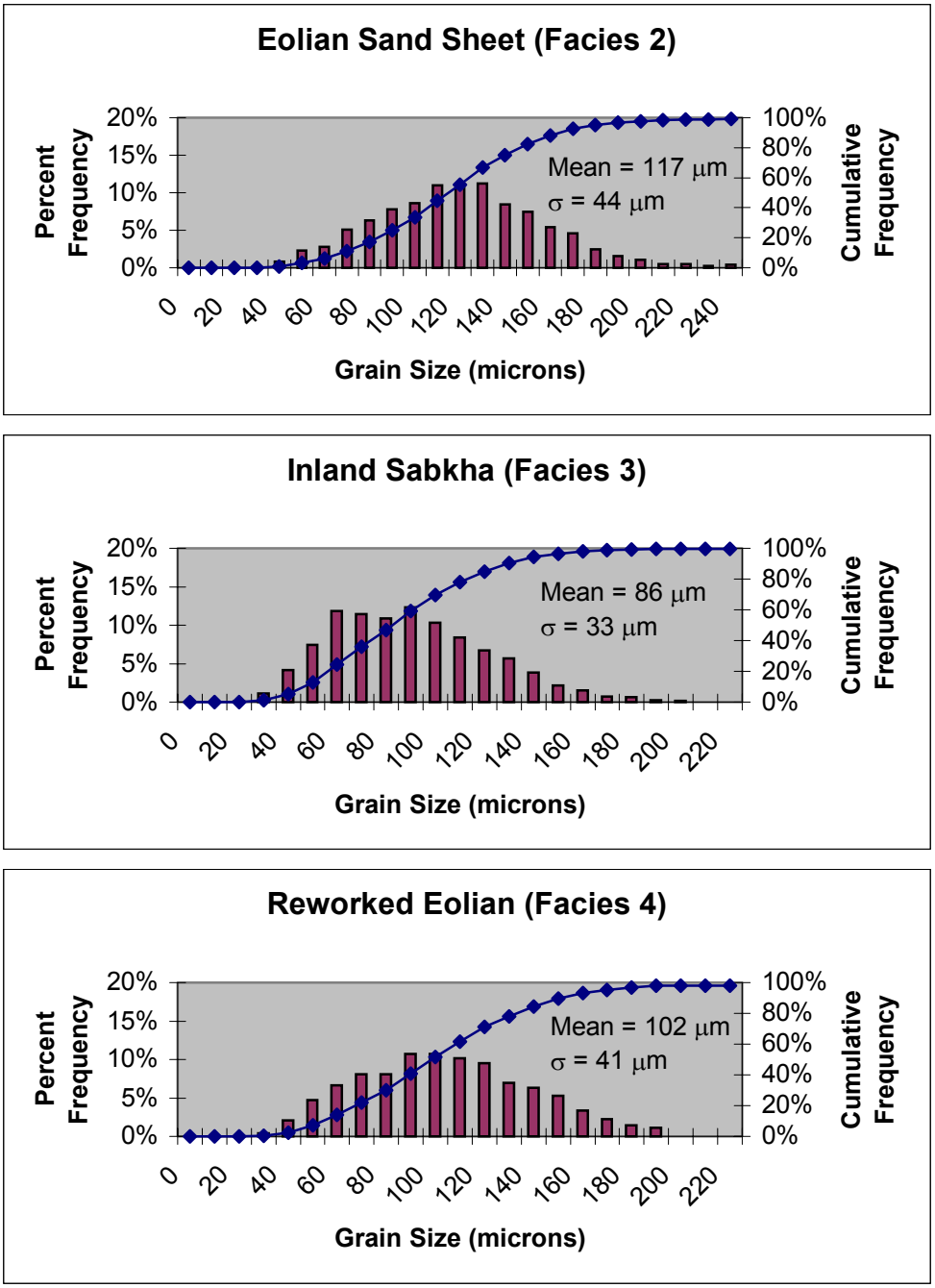

Figure 20. Frequency distributions for eolian sand sheet, inland sabkha, and reworked eolian depositional environments.

mean of 75 microns, 3.74ϕ) was deposited in a low energy environment wherein ephemeral streams released their suspension load to form these fine-grained deposits.

Composition

Detrital Composition

The Shattuck Sandstone is arkosic to sub-arkosic based on Folk's (1968) classification scheme (Fig. 21). Average detrital components are: 76% monocrystalline quartz, 22% feldspar, and 2% rock fragments and accessories. Monocrystalline quartz comprises 65 to 85% of the detrital mineral grains, and feldspars constitute 10 to 35%. Most of the feldspars are potassium feldspars, and plagioclase is present in minor amounts.

Rock fragments and accessory minerals comprise a small percentage of the detrital composition (less than 7% for all samples). The majority of rock fragments are metamorphic polycrystalline quartz, and mudstone clasts are also present in rare amounts. Mudstone clasts could have been derived from intraformational sediments of the surrounding environments.

Common accessory minerals include micas such as chlorite and muscovite, opaque iron oxide minerals, and clay minerals that are unidentifiable under a petrographic microscope. The micas are usually abundant in silty mud drapes found within the various facies.

Major Cements and Matrix Minerals

The majority of cementing minerals found in the Shattuck Sandstone are anhydrite and dolomite (average: 19% anhydrite and 8% dolomite of total rock

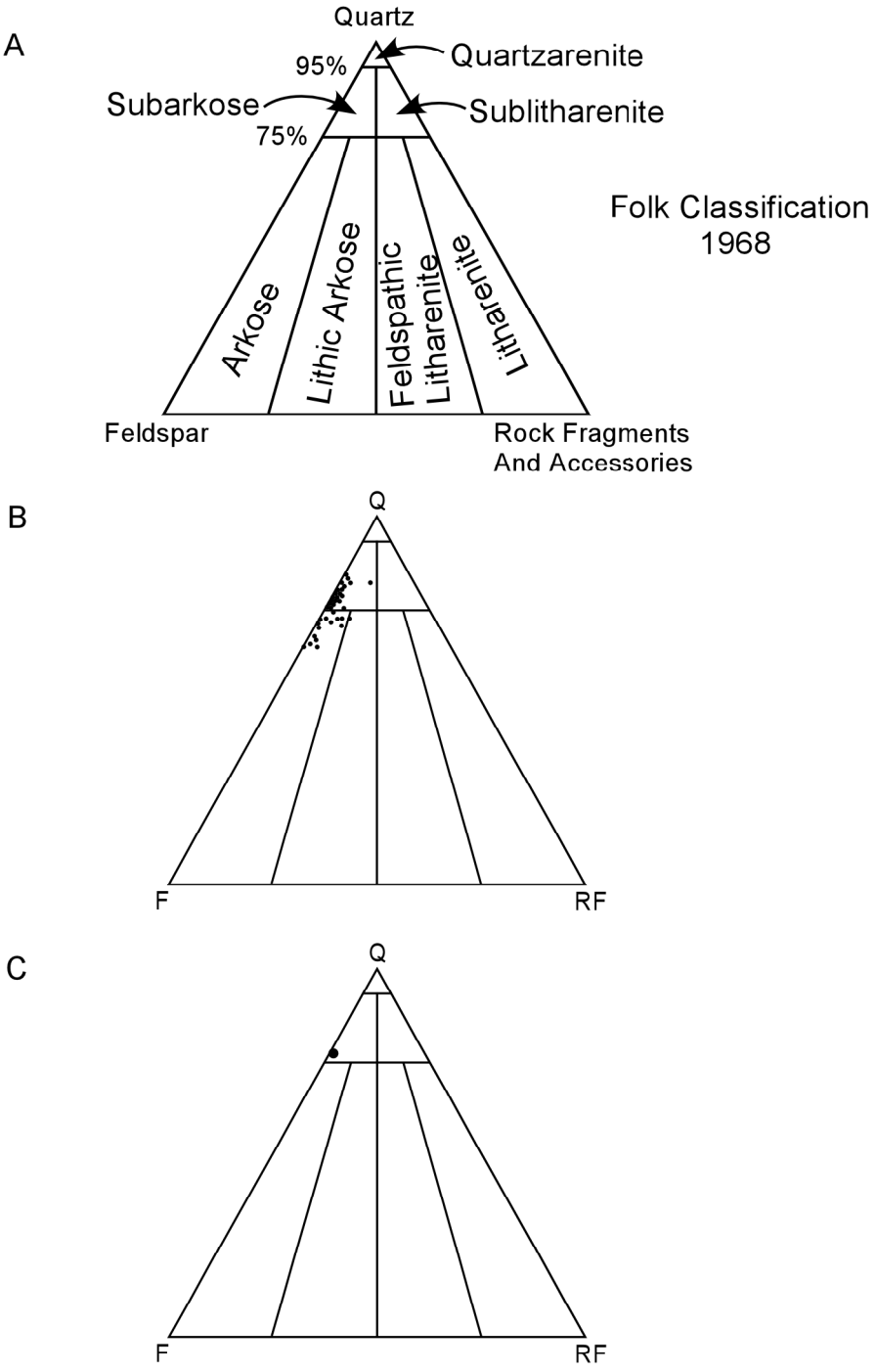

Figure 21. Ternary diagrams. (A) Ternary classification scheme from Folk, 1968. (B) Composition plots for all samples. (C) Plot of average composition of all samples.

composition respectively). Anhydrite is the dominant cement in all facies, except within Facies 4 (Fig. 22), which is dominated by dolomite cement.

Anhydrite cements are pore-filling and coarse-grained or poikilotopic in nature (Fig. 23A). It is found in all facies, but is exceptionally abundant in the finer-grained facies such as Subfacies 1A (27% total rock composition), Subfacies 1C (33% total rock composition), and Facies 3 (38% total rock composition).

Dolomite cement occurs both as an anhedral, finely crystalline pore-filler and as a poikilotopic (coarse-grained) pore-filler (Fig. 23B). Dolomite cement is present in all facies in minor amounts, except Facies 2 and Facies 4 where it is found in abundance.

Hydrocarbon residue or "dead oil" is found with the pore space and lining grains within parts of the reservoir section (Fig. 23C). This residue is defined as residual oil by Levandowski et al., (1973).

Gypsum was also observed in thin section, although in minor amounts (<1%). It occurs as a poikilotopic pore-filler and has a fibrous appearance (Fig. 23D). It is always found in conjunction with the poikilotopic anhydrite cement.

Hematite cement is responsible for the red coloration of some deposits. It is most often found lining grains, and is filling pores in rare instances. The amount of hematite cement was difficult to quantify because it is generally present thinly coating grains, and diffused in pore-filling cements.

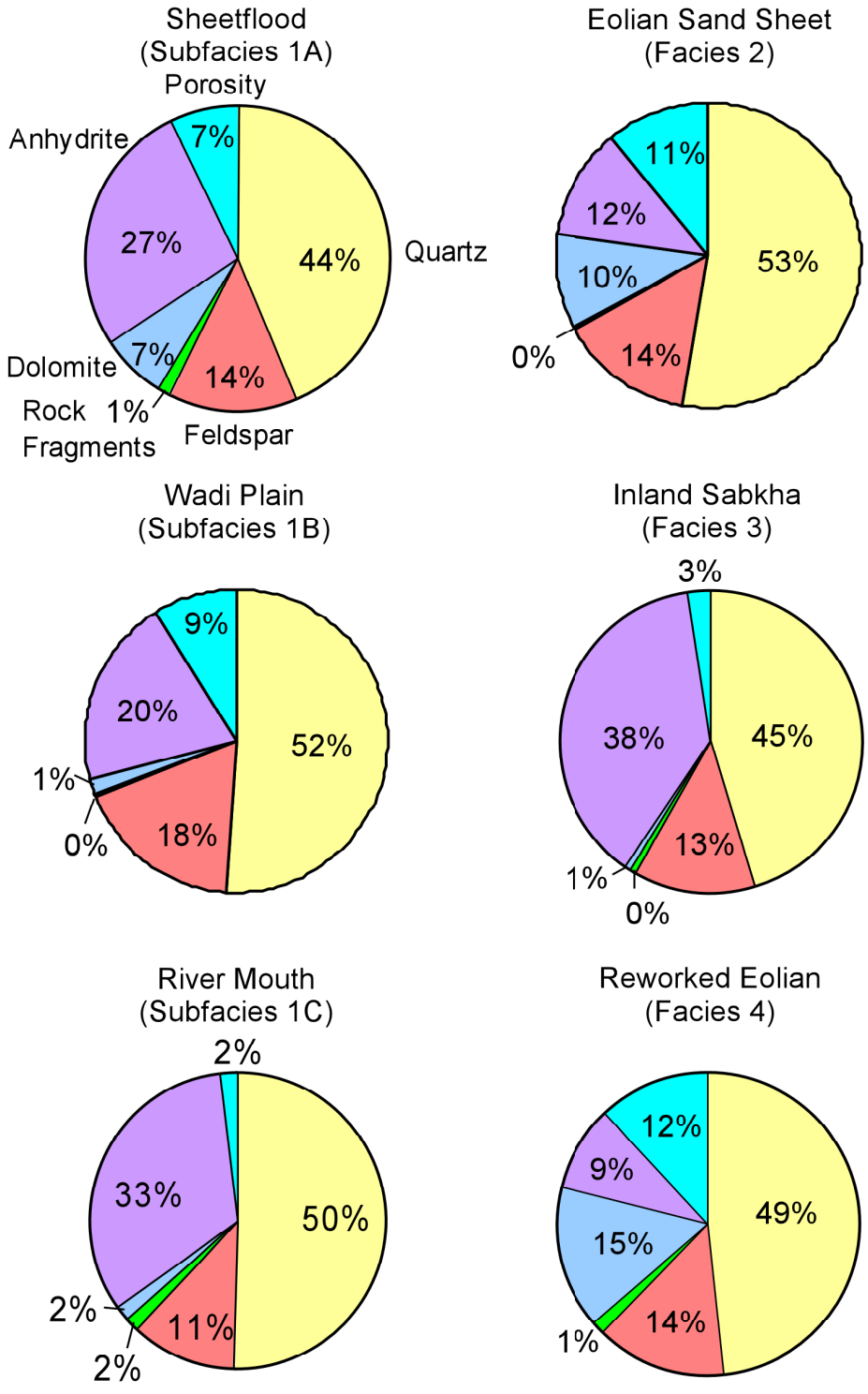

Figure 22. Pie diagrams showing total rock composition for each facies of the Shattuck Sandstone.

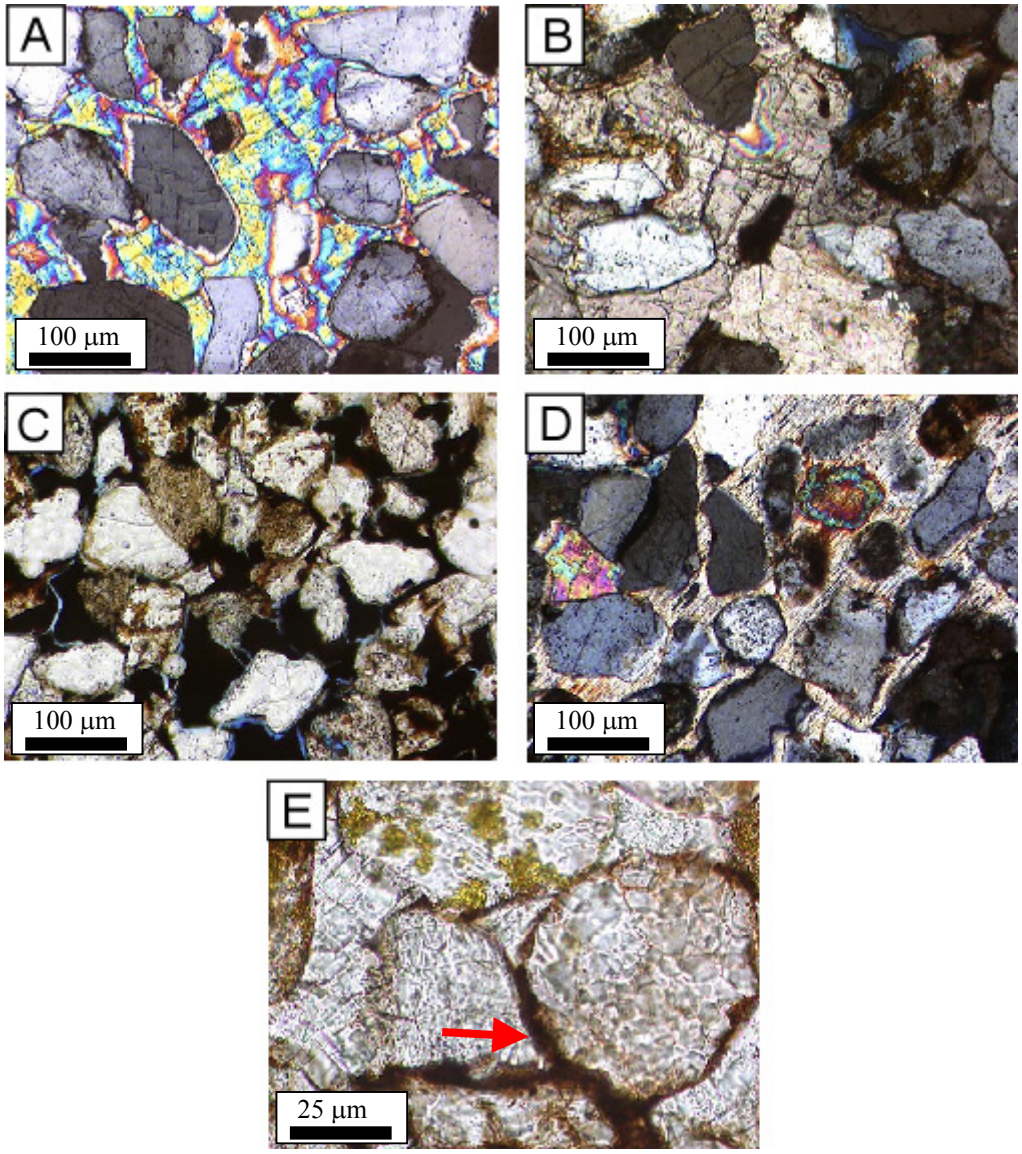

Figure 23. Photomicrographs illustrating cement textures. (A) Poikilotopic anhydrite cement. (B) Poikilotopic dolomite cement. (C) Pores containing dead oil. (D) Gypsum (fibrous appearance) and anhydrite (high birefringence) cement. (E) Hematite as a grain-liner.

Diagenetic History

The diagenetic history of the Shattuck Sandstone can be divided into an early stage immediately following deposition, and a late stage of dissolution prior to hydrocarbon migration. During the early diagenetic stage, there was partial to complete dissolution labile framework grains, such as plagioclase feldspars, ferromagnesian silicates (e.g. pyroxenes, hornblende), and heavy minerals (e.g. magnetite, ilmenite). Evidence for this stage of diagenesis includes partially to completely oxidized grains, voids completely or partially filled by late-stage cementation, and corrosion of plagioclase feldspars. The diagenetic history for the Shattuck Sandstone is illustrated in figure 24.

Also common to this early stage of diagenesis was the mechanical infiltration of clays by meteoric water, mechanical compaction of sediments, and eventually the precipitation of hematite. In the inland sabkha facies, hematite is found lining grains and acting as meniscus bridges between grain-to-grain contacts (Fig. 23E). Clay minerals, initially infiltrated by meteoric waters, form a geopetal fabric within the host grain framework (Crone, 1974; Walker, 1976). As clays continue to be infiltrated, they envelope the entire grain (Walker, 1976). If the clays or other surrounding minerals contain iron, the oxygen-rich pore water will eventually cause hydrolysis to occur. This allows iron to be released in solution, which is later precipitated as red-colored hematite or other iron oxide minerals (Walker, 1976).

The last early stage diagenetic event was the precipitation of anhydrite and dolomite cements. Hematite is dispersed throughout a portion of the cements in places,

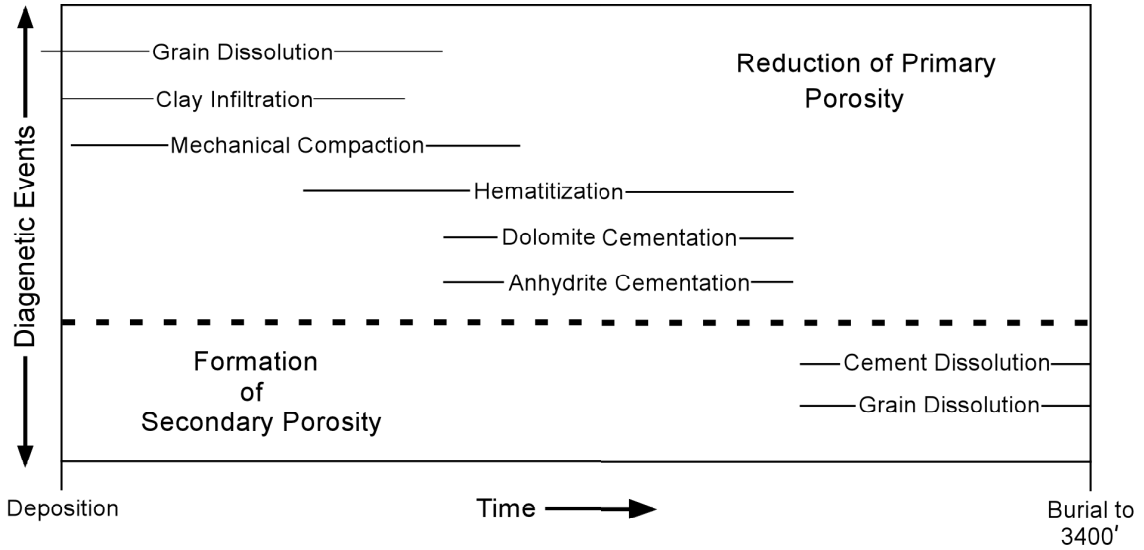

Figure 24. Diagram illustrating the diagenetic events of the Shattuck Sandstone.

which suggests hematite precipitation was partly contemporaneous with the formation of anhydrite and dolomite cements. Anhydrite is not stable at the surface, except under special circumstances. It is likely that gypsum cements precipitated, which later converted to anhydrite in the subsurface. Likewise, dolomite cements were more likely to have been precipitated as calcite or aragonite, and then later converted to dolomite.

Anhydrite and dolomite often occur together, but one mineral is usually dominant for a given facies. Dolomite is present in minor amounts or is absent in all facies except for Facies 2 (eolian sand sheet) and Facies 4 (reworked eolian) where it is more abundant, if not dominant. One explanation to this occurrence is that the rates of evaporation within the continental environments (inland sabkha and fluvial environments) were higher than those environments closer to the coastal areas. These continental environments are then sites of brine formation. Another explanation lies in the groundwater chemistry. The groundwater of the coastal environments is recharged

with lagoonal waters, which have a higher concentration of calcium carbonate than groundwater underlying the continental environments.

Late stage diagenesis involved grain dissolution, decementation, and bleaching of various parts of the Shattuck Sandstone, mainly the more permeable reservoir facies. This stage occurred prior to hydrocarbon migration, and resulted in the formation of both intragranular and intergranular porosity.

Secondary porosity was identified using the criteria of Schmidt and McDonald (1979b). Secondary porosity is evidenced by: (1) partial dissolution of feldspars forming intra-granular porosity (Fig. 25A and B); (2) partial dissolution of cement matrix forming corrosive edges around the cement and resulting in inter-granular porosity (Fig. 25B and D); (3) oversized pore textures (Fig. 25C); and (4) inhomogeneity of packing (Fig. 25C).

Formation of secondary porosity by the dissolution of cement is common in other sandstones containing anhydrite cement. Markert and Al-Shaieb (1984), reported secondary porosity by anhydrite dissolution in the upper, Permian portion of the Minnelusa Formation in the Powder River Basin, Wyoming. Schenk and Richardson (1985) also reported secondary porosity due to anhydrite dissolution within both the Minnelusa Formation (Wyoming) and the San Andres Limestone of southeastern New Mexico. Decementation and framework grain dissolution (e.g. feldspars) in later diagenetic stages is believed to be a natural consequence of diagenesis, whereby organic acids and carbon dioxide are released during the maturation of organic material (Schmidt and McDonald, 1979a; Siebert et al., 1984; Surdam et al., 1984; Surdam et al., 1989).

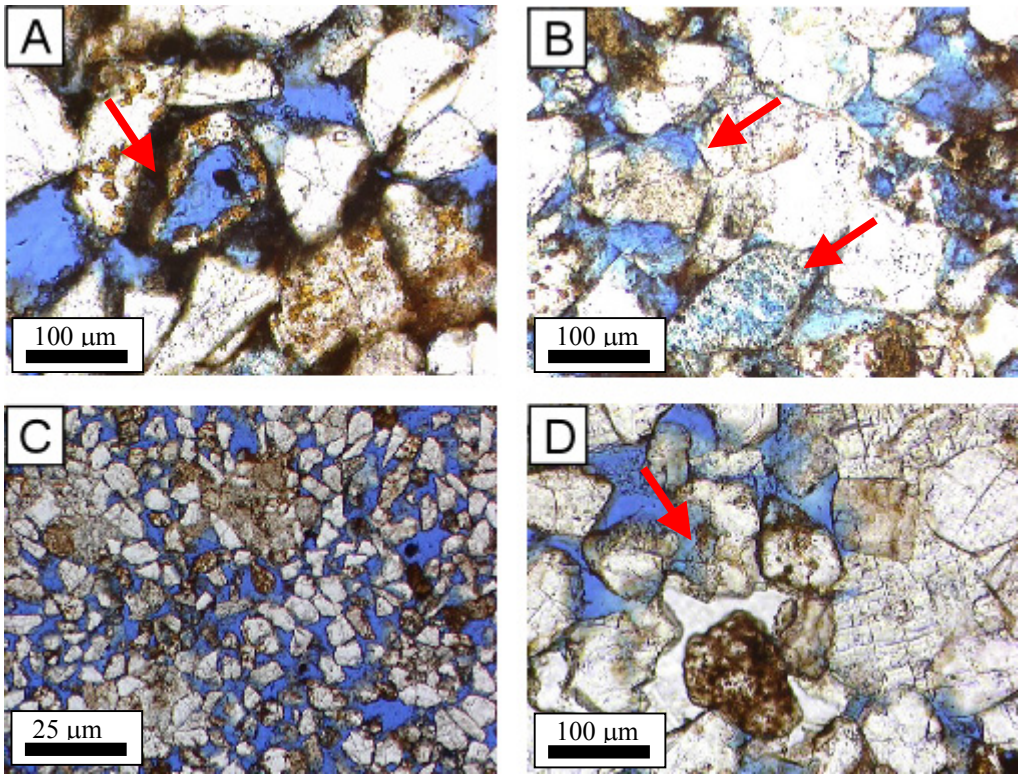

Figure 25. Photomicrographs illustrating diagenetic features of secondary porosity. (A) Arrow indicates partial dissolution of potassium feldspar grain forming intra-granular porosity. (B) Upper arrow indicates partial cement dissolution; lower arrow shows honeycombed grain that resulted from partial dissolution. (C) Photomicrograph illustrating both oversized pores and inhomogeneity of packing. (D) Arrow indicates partial cement dissolution.

Reservoir facies within the Shattuck Sandstone exhibit a tan or drab coloring, whereas the nonreservoir facies are dark reddish-brown. In adjacent dry holes, however, the reservoir facies are reddish-brown coloration with only thin streaks of tan coloration. Bleaching of the reservoir rock is not only an attribute present in the Shattuck Sandstone, but is common to other hydrocarbon-bearing sandstones as well. Levandowski et al., (1979) noted a similar discoloration of the Lyons Sandstone of the Denver Basin. Moulton (1926) also had similar findings in the Chugwater sandstone of southern Montana. Levandowski et al., (1979) attributes this bleaching effect to the reduction and removal of soluble iron by contact with organic matter. The same is true for this study given that the bleaching is only present where hydrocarbons, or hydrocarbon residues, are found.

RESERVOIR CHARACTERISTICS

Reservoir units in the Shattuck Sandstone at Mesa Queen Field include wadi plain, eolian sand sheet, and reworked eolian facies. These facies have higher porosities, coarser average grain size, and lower average mud content, and lack mud laminae. A commercially prepared core analysis (Fig. 26) shows porosity, horizontal permeability, oil saturation, and water saturation changes relative to a lithostratigraphic log. The samples were taken at 1 ft (0.3 m) intervals throughout the core. Also shown in figure 26 is porosity obtained by point counting methods.

The petrophysical properties of reservoir facies differ drastically from those of nonreservoir facies. The reservoir is clearly defined by these changes, and thus can be classified as a facies-selective diagenetic trap. Facies selective diagenetic traps are those in which reservoir facies follow depositional environments or subenvironments (Fryberger, 1986). Nonreservoir facies (sheetflood, inland sabkha, and river mouth) underwent a higher degree of cementation than the reservoir facies. Facies along the Arabian Gulf are a modern example of how facies-selective diagenetic traps form. There, eolian sabkha and interdune facies exhibit early cementation to a greater extent than dune and sand sheet facies. Early cementation of eolian sabkha and interdune facies is attributed to the close proximity of these facies to evaporites in the groundwater table and marine waters.

Core porosities of all sandstone facies (bounding facies excluded) range from 5.9 to 30.1%, and average 16.4%. Porosities obtained from thin sections range from 0.5 to 28.6% and average 9.1%. Thus, it could be said that porosity values obtained from thin

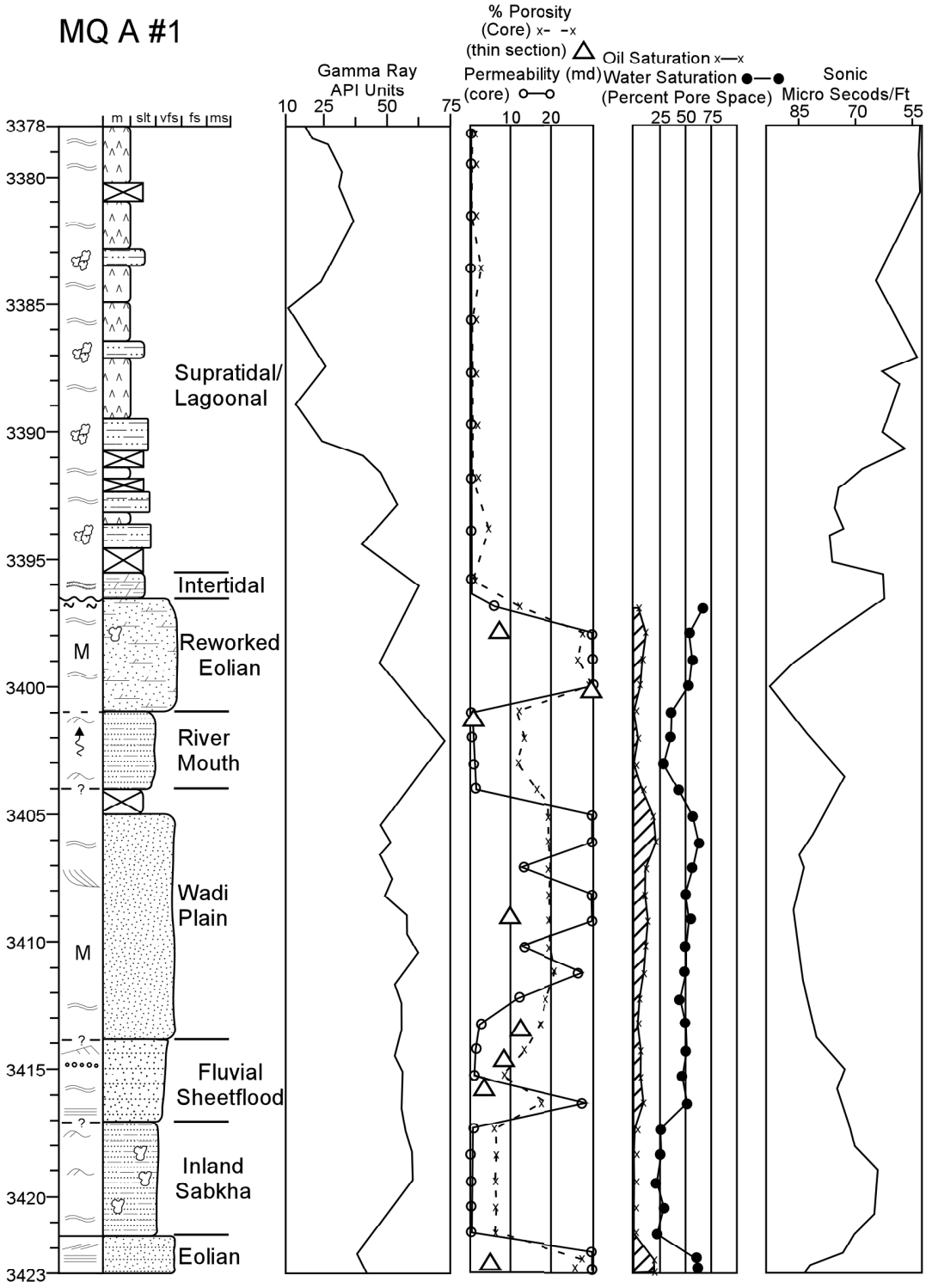

Figure 26. Lithostratigraphic column with petrophysical data. Note that horizontal permeability values are off the scale in many cases.

sections under estimate porosity when compared to core porosity. However this is not a valid comparison since thin sections and core plugs were sampled at different intervals within the core. The core analysis also had a shorter sampling interval compared to thin sections, which were taken at irregular intervals.

Horizontal permeability values of the Shattuck Sandstone range from less than 0.1 md to1006 md, and average 117 md. Reworked eolian and eolian sand sheet facies have the highest porosity and permeability values, whereas river-mouth and inland sabkha facies have the lowest values. A crossplot of porosity vs permeability (Fig. 27) indicates a correlation between these properties. The crossplot does show that reservoir facies yield higher porosity and permeability values than the nonreservoir facies, which show measurable porosity values with very little permeability. Porosity values obtained from thin section for the nonreservoir facies are near zero in many cases. Core porosities for the nonreservoir facies, however, are much higher (Fig. 22). This may indicate microporosity within the nonreservoir facies, which would account for the low permeability values for these facies.

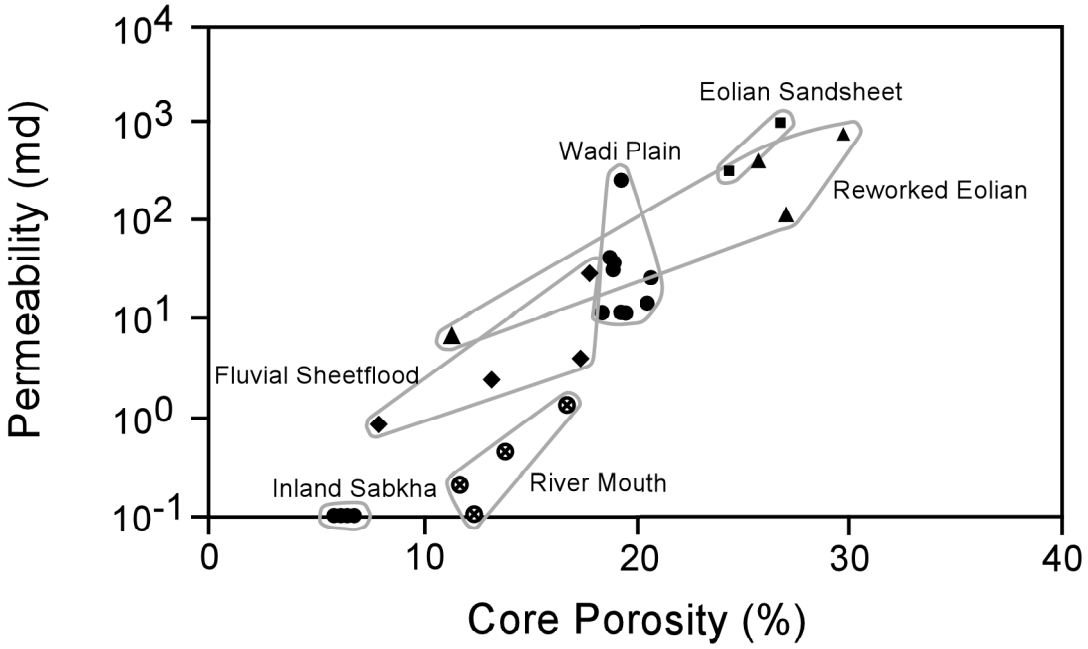

Figure 27. Crossplot of porosity vs permeability for the MQA #1 well.

REGIONAL SYNTHESIS

Changes in the Shattuck Sandstone on a broader scale can be defined by comparing the successions observed at Mesa Queen Field with those observed in two nearby fields; South Caprock (Malicse, 1988) and Central Corbin (Siegel, 1989). South Caprock lies approximately five miles to the northwest of Mesa Queen and is the southern extent of the large Caprock Field. Central Corbin lies approximately ten miles to the southeast of Mesa Queen Field.

Malicse (1988) suggested that the Shattuck Sandstone at South Caprock was deposited in three environments: fluvial sandflats, inland sabkhas, and eolian sand sheets. Siegel (1989) suggested that the Shattuck Sandstone was deposited in two environments: inland sabkhas and eolian sand sheets. In both studies, the depositional environments of the bounding facies were coastal sabkha and lagoonal. Figure 28 shows a generalized cross-section intersecting all three fields, and illustrates facies changes in the Shattuck Sandstone.

Although depositional facies observed in the three fields are similar, there are some differences. First, the northern part of the Northwest Shelf is dominated by fluvial deposits, whereas the southern and more basinward parts of the Shattuck Sandstone lack fluvial deposits and are dominated by inland sabkha and eolian sand sheet deposits. The lack of fluvial deposits in the southern portion of the Northwest Shelf indicates insufficient time for fluvial sediments to prograde across the entire shelf. Secondly, depositional environments of the uppermost facies vary in the different field areas. At South Caprock this uppermost interval was interpreted to be river-mouth deposits of a

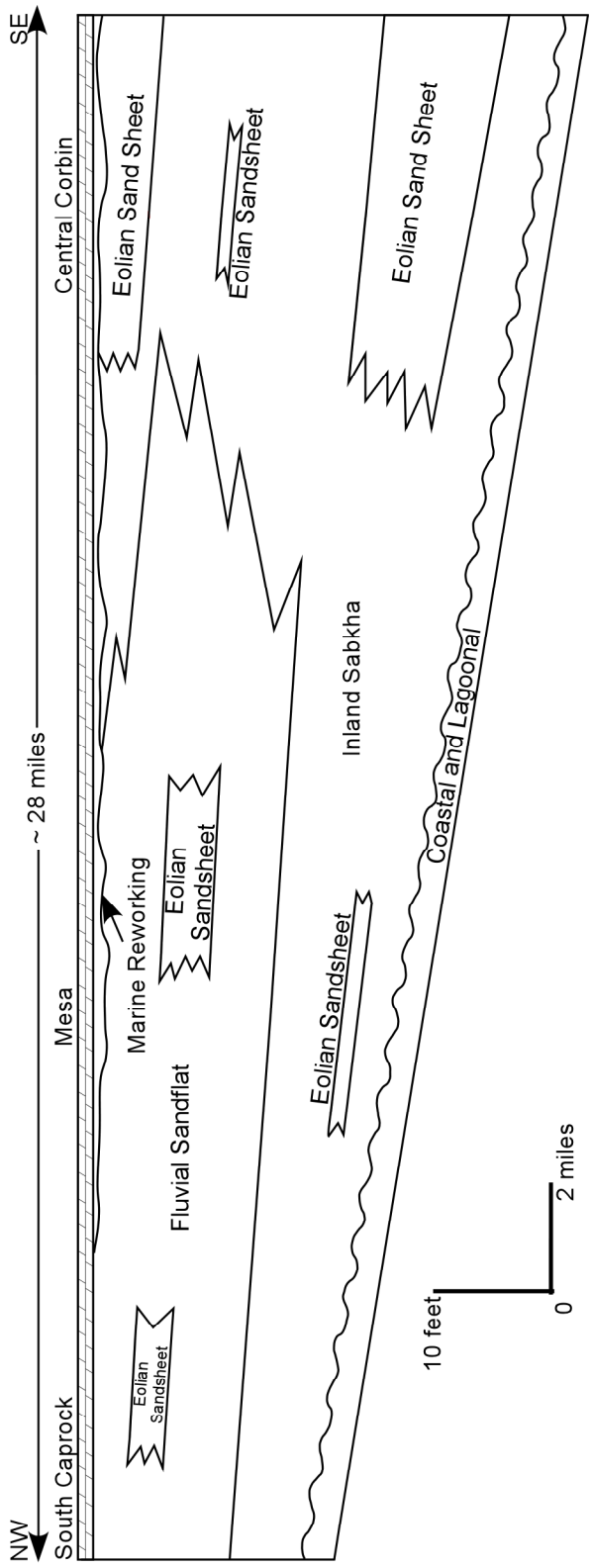

Figure 28. Generalized dip cross-section illustrating facies changes of the Shattuck Sandstone.

fluvial sandflat. At Central Corbin this interval varies from inland sabkha to eolian sand sheet deposits. At Mesa Queen, marine-reworked eolian sand is occupies this interval. This reworked eolian facies is either restricted to the Mesa Queen Field area or previous interpretations misidentified the depositional environment. Marine processes that rework sediments act over large areas, and the evidence at the top of the Shattuck Sandstone should be widespread, not locally confined to the Mesa Field area. Lastly, the dolomicrite seen capping the Shattuck Sandstone in all three fields was previously interpreted to be lagoonal, in contrast to the intertidal interpretation suggested by this study.

Thickness changes across the Shattuck Sandstone refine a regional basinward-thickening. At South Caprock, the thickness ranges from 18-23 feet (5.5-7.0 m), at Mesa from 20-36 feet (6.1-11.0 m), and at Central Corbin from 54-64 feet (16.5-19.5 m). All three fields are the result of a stratigraphic trap formed on a gently dipping homocline, and the Shattuck Sandstone exhibits a local thickening within these field areas (Fig. 29). Also, the three fields exhibit elongate sand-body geometry. Table 2 summarizes Shattuck Sandstone and reservoir properties for each field area.

Many studies of shelf, shelf margin, and basinal sediments of the Permian Basin have attempted to establish a sequence stratigraphic framework for these cyclic deposits. These studies concentrated on exposures in the Guadalupe Mountains where shelf to basin deposits are well exposed. The Queen Formation has been interpreted to be bounded by sequences related to high frequency sea-level changes (Kerans, 1995). Like other formations of the Artesia Group, the Queen Formation contains numerous cycles

of interbedded siliciclastics, carbonates, and evaporites. The Shattuck Sandstone and its bounding facies are one of the more prominent cycles in the Artesia Group. Smaller, higher frequency cycles within the Queen Formation could be the result of minor sea-level fluctuations. Because of the slope of the shelf, minor changes in climate, sea level, sediment supply, or subsidence rates could result in a major shift in facies across the shelf.

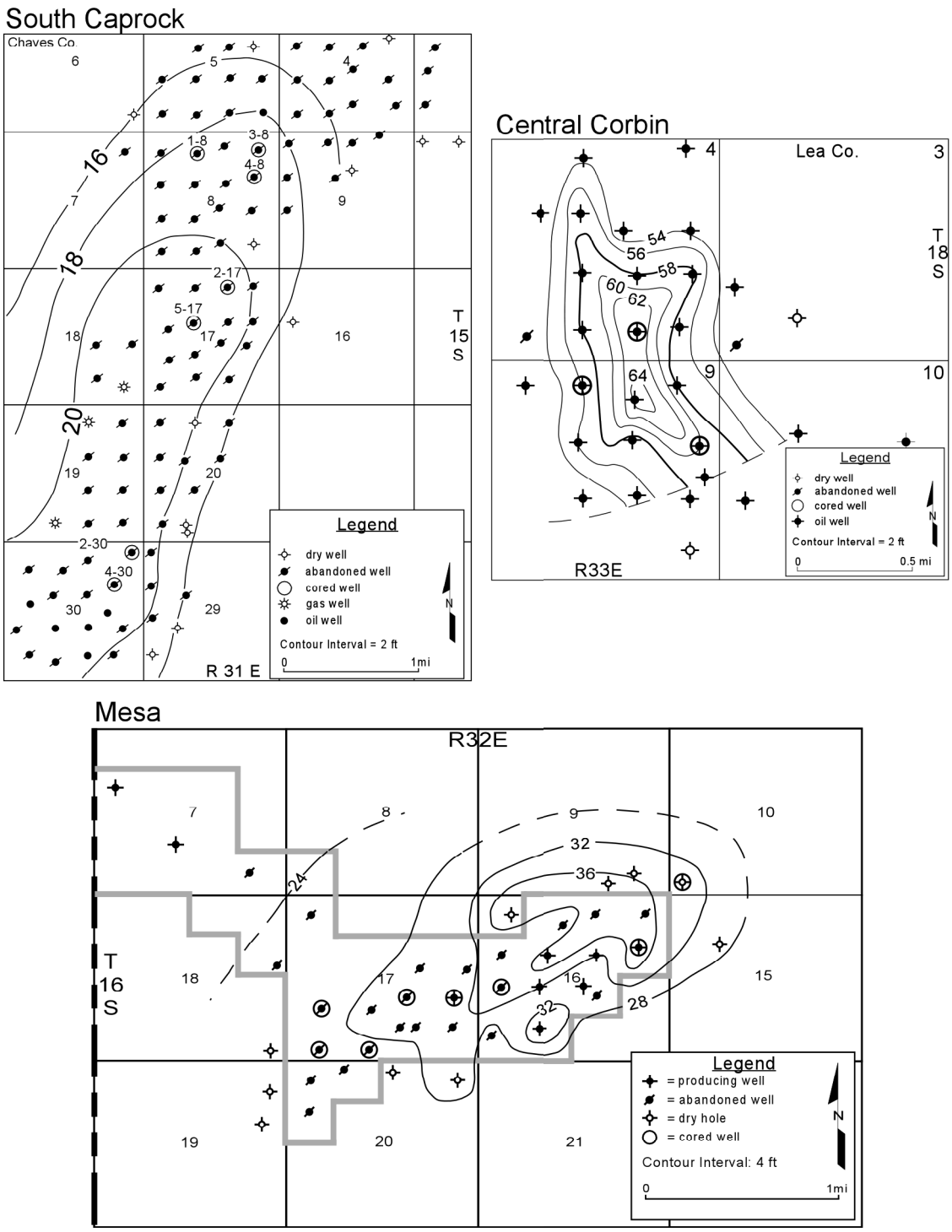

Figure 29. Isopach maps of the Shattuck Sandstone for all three field areas.

Table 2. Regional properties of the Shattuck Sandstone.

Field	Depositional Environments	Reservoir Facies	Dip (ft/mi)	Shattuck Thickness (ft)	Reservoir Porosity (%)	Reservoir Permeability (md)
South Caprock	fluvial sandflat, eolian sand sheet, inland sabkha	fluvial sandflat , eolian sand sheet	80 (0.9º)	18-23	15-20	5-360
Mesa	fluvial sandflat, eolian sand sheet, inland sabkha	fluvial sandflat, eolian sand sheet, reworked eolian	37 (0.4º)	20-36	3-29	3.9-1006
Central Corbin	inland sabkha, eolian sand sheet	eolian sand sheet	120 (1.3º)	54-64	5-16	0.55-82

CONCLUSIONS

This study characterizes the Shattuck Sandstone at Mesa Queen Field to interpret depositional environments and refine models of reservoir quality. These results are compared with those from two previous studied nearby fields to define a broader depositional framework for the Shattuck Sandstone.

The Shattuck Sandstone was deposited in four siliciclastic environments during a lowstand of sea level: (1) fluvial sandflats, (2) eolian sand sheets, (3) inland sabkhas, and (4) marine-reworked eolian sands. The fluvial sandflat facies was further divided into sheetflood, wadi plain, and river-mouth deposits. The Shattuck Sandstone is bounded above and below by dolomicrites, evaporites, and siliciclastics deposited in coastal sabkha and lagoonal environments.

The Shattuck Sandstone is very fine-grained, moderately well-sorted subarkose. Cements include anhydrite and dolomite, with lesser amounts of gypsum and hematite. Organic acids produced during hydrocarbon maturation caused decementation and grain dissolution throughout the Shattuck Sandstone forming both intergranular and intragranular secondary porosity. Due to extensive, early cementation within the inland sabkha, river-mouth, and sheetflood facies, reservoirs are confined to wadi plain, eolian, and marine-reworked eolian facies. This, and the lack of structural closure, indicates the reservoir is defined by a facies-selective diagenetic trap.

Regionally, the Shattuck Sandstone is a basinward-thickening sheet sand. All three fields studied occur on locally-thickened, elongate sand bodies oriented at high angles to the paleocoastline. The thickness and orientation of these sand bodies appears

to be a factor in reservoir formation, but this is not well understood. Facies of the Shattuck Sandstone across the Northwest Shelf record the progradation of fluvial sediments over pre-existing inland sabkhas. The lack of fluvial facies in the southern portion of the Northwest Shelf illustrates the short-lived nature of these fluvial sediments due to the ensuing highstand of sea level. Fluvial processes were important in delivering sediment from source areas to the shelf. However, sabkha and eolian systems dominated areas more basinward on the shelf, and it seems likely that eolian processes were important in delivering sediment to the coastal areas.

REFERENCES CITED

AAPG, 1983c, COSUNA–Southwest/Southwest Mid-Continent Correlation Chart, J. H. Hills and F. E. Kottlowski, coordinators.

Ahlbrandt, T. S., and S. G. Fryberger, 1982, Introduction to eolian deposits, *in* P. A. Scholle and D. R. Spearing, eds., Sandstone depositional environments: AAPG Memoir 31, p. 11-47.

Andreason, M. W., 1992, Coastal siliciclastic sabkhas and related evaporative environments of the Permian Yates Formation, North Ward-Estes Field, Ward County, Texas: AAPG Bulletin, v. 76, p. 1735-1759.

Ball, S. M., J. W. Roberts, J. A. Norton, and W. D. Pollard, 1971, Queen Formation (Guadalupian, Permian) outcrops of Eddy County, New Mexico, and their bearing on recently proposed depositional models: AAPG Bulletin, v. 55, p. 1348-1355.

Chan, M. A., and G. Kocurek, 1988, Complexities in eolian and marine interactions: processes and eustatic controls on erg development: Sedimentary Geology, v. 56, p. 283-300.

Chayes, F., 1949, A simple point-counter for thin-section analysis: American Mineralogist, v. 34, p. 1-11.

Crandall, K. H., 1929, Permian stratigraphy of southeastern New Mexico and adjacent parts of west Texas: AAPG Bulletin, v. 13, p. 927-944.

Crone, A. J., 1974, Experimental studies of mechanically-infiltrated clay matrix in sand (abs.): Geological Society of America Abstracts with Programs, v. 6, p. 701.

Dott, R. H., Jr., and C. W. Byers, 1981, SEPM Research Conference on modern shelf and ancient cratonic sedimentation–the orthoquartzite-carbonate suite revisited: Journal of Sedimentary Petrology, v. 51, p. 329-347.

Dott, R. H., Jr., C. W. Byers, G. W. Fielder, S. R. Stenzel, and K. E. Winfree, 1986, Aeolian to marine transition in Cambro-Ordovician cratonic sheet sandstones of the northern Mississippi Valley, U.S.A.: Sedimentology, v. 33, p. 345-367.

Folk, R., 1968, Petrology of sedimentary rocks: Austin, Texas, Hemphill, 170 p.

Folk, R., 1974, Petrology of sedimentary rocks: Austin, Texas, Hemphill, 182 p.

Fryberger, S. G., T. S. Ahlbrandt, and S. Andrews, 1979, Origin, sedimentary features, and significance of low-angle eolian "sand sheet" deposits, Great Sand Dunes National Monument and vicinity, Colorado: Journal of Sedimentary Petrology, v. 49, p.733-746.

Fryberger, S. G., A. M. Al-Sari, and T. J. Clisham, 1983, Eolian dune, interdune, sand sheet, and siliciclastic sabkha sediments of an offshore prograding sand sea, Dharan area, Saudi Arabia: AAPG Bulletin, v. 67, p. 280-312.

Fryberger, S. G., 1986, Stratigraphic traps for petroleum in wind-laid rocks: AAPG Bulletin, v. 70, p. 1765-1776.

Galley, J. E., 1958, Oil and geology in the Permian Basin of Texas and New Mexico, *in* L. G. Weeks, ed., Habitat of oil, a symposium: Tulsa, AAPG, p. 395-446.

Glagolev, A. A., 1934, Quantitative analysis with the microscope by point method: Engineering Mining Journal, v. 135, p. 399.

Glennie, K. W., 1970, Desert sedimentary environments: Developments in sedimentology 14: Amsterdam, Elsevier, 222 p.

Hardie, L. A., J. P. Smoot, and H. P. Eugster, Saline lakes and their deposits: a sedimentological approach, *in* A. Matter and M. E. Tucker, eds., Modern and ancient lake sediments: International Association of Sedimentologists Special Publication 2, p. 7-41.

Hills, J. M., 1972, Late Paleozoic sedimentation in west Texas Permian Basin: AAPG Bulletin, v. 56, p. 2303-2322.

Hills, J. M., 1985, Structural evolution of the Permian Basin of west Texas and New Mexico, *in* P. W. Dickerson, and W. R. Muehlburger, eds., Structure and tectonics of trans-Pecos Texas: West Texas Geological Society Field Conference Publication 85-81, p. 89-99.

Hunter, R. E., 1977, Basic types of stratification in small eolian dunes: Sedimentology, v. 24, p. 361-387.

Kerans, C., 1995, Use of one- and two-dimensional cycle analysis in establishing high-frequency sequence frameworks, *in* J. F. Read, C. Kerans, L. J. Weber, J. F. Sarg, and F. M. Wright, eds., Milankovitch sea-level changes, cycles, and reservoirs on carbonate platforms in greenhouse and ice-house worlds: SEPM Short Course Notes 35, part 2, p. 1-20

Kinsman, D. J. J., 1969, Modes of formation, sedimentary associations, and diagnostic features of shallow-water and supratidal evaporites: AAPG Bulletin, v. 53, p. 830-840.

Kocurek, G., and R. H. Dott, Jr., 1981, Distinctions and uses of stratification types in the interpretation of eolian sand: Journal of Sedimentary Petrology, v. 51, p. 579-595.

Kocurek, G., and J. Nielson, 1986, Conditions favourable for the formation of warm-climate aeolian sand sheets: Sedimentology, v. 33, p. 795-816.

Levandowski, D. W., M. E. Kaley, S. R. Silverman, and R. G. Smalley, 1973, Cementation in the Lyons Sandstone and its role in oil accumulation, Denver Basin, Colorado: AAPG Bulletin, v. 57, p. 2217-2244.

Lowe, D. R., 1975, Water escape structures in coarse-grained sediments: Sedimentology, v. 22, p. 157-204.

Lowenstein, T. K., and L. A. Hardie, 1985, Criteria for the recognition of salt-pan evaporites: Sedimentology, v. 32, p. 627-644.

Malicse, A., 1988, The environment of deposition and diagenesis of the Shattuck Member of the Queen Formation (Guadalupian, Permian) at Caprock Queen Field, Chaves County, New Mexico: Master's thesis, Texas A&M University, College Station, Texas, 160 p.

Malicse, A., and Mazzullo, J., 1990, Reservoir properties of the desert Shattuck Member, Caprock Field, New Mexico, *in* J. H. Barwis, J. G. McPherson, and J.R. J. Studlick, eds., Sandstone petroleum reservoirs: New York, Springer-Verlag, p. 133-152.

Markert, J. C., and Z. Al-Shaieb, 1984, Diagenesis and evolution of secondary porosity in upper Minnelusa Sandstones, Powder River Basin, Wyoming, *in* D. A. McDonald and R. C. Surdam, eds., Clastic diagenesis: AAPG Memoir 37, p. 367-389.

Mazzullo, J., A. Malicse, and J. Siegel, 1991, Facies and depositional environments of the Shattuck Sandstone on the Northwest Shelf of the Permian Basin: Journal of Sedimentary Petrology, v. 61, p. 940-958.

McKee, E. D., E. J. Crosby, and H. L. Berryhill, Jr., 1967, Flood deposits, Bijou Creek, Colorado, June 1965: Journal of Sedimentary Petrology, v. 37, p. 829-851.

Meissner, F. F., 1972, Cyclic sedimentation in middle Permian strata of the Permian Basin, west Texas and New Mexico, *in* J. C. Elam and S. Chuber, eds., Cyclic sedimentation in the Permian Basin, 2nd edition: West Texas Geological Society Publication 72-60, p. 203-232.

Moran, W. R., 1954, Proposed type sections for the Queen and Grayburg Formations of Guadalupe age in the Guadalupe Mountains, Eddy County, New Mexico (abs.): Geological Society of America Bulletin, v. 65, p. 1288.

Moulton, G. F., 1926, Some features of red bed bleaching: AAPG Bulletin, v. 10, p. 304-311.

Pray, L. C., 1977, The all wet, constant sea-level hypothesis of Upper Guadalupian shelf and shelf-edge strata, Guadalupe Mountains, New Mexico and Texas (abs.), *in* M. E. Hileman and S. J. Mazzullo, eds., Upper Guadalupian facies, Permian reef complex, Guadalupe Mountains, New Mexico and west Texas: Permian Basin Section SEPM Publication 77-16, v. 1, p. 433.

Reese, R. S., 1984, Stratigraphy of the Entrada Sandstone and Todilto Limestone (Jurassic), north-central New Mexico: Master's thesis, Colorado School of Mines, Golden, Colorado, 184 p.

Saller, A. H., P. M. Harris, B. L. Kirkland, and S. J. Mazzullo, 1999, Geologic framework of the Capitan depositional system–previous studies, controversies, and contents of this special publication, *in* A. H. Saller, P. M. Harris, B. L. Kirkland, and S. J. Mazzullo, eds., Geologic framework of the Capitan reef: SEPM Special Publication 65, p. 1-13

Schenk, C. J., and R. W. Richardson, 1985, Recognition of interstitial anhydrite dissolution: a cause of secondary porosity, San Andres Limestone, New Mexico, and upper Minnelusa Formation, Wyoming: AAPG Bulletin, v. 69, p1064-1076.

Schmidt, V., and D. A. McDonald, 1979a, The role of secondary porosity in the course of sandstone diagenesis, *in* P. A. Scholle and P. R. Schluger, eds., Aspects of diagenesis: SEPM Special Publication 26, p. 175-207.

Schmidt, V., and D. A. McDonald, 1979b, Texture and recognition of secondary porosity in sandstones, *in* P. A. Scholle and P. R. Schluger, eds., Aspects of diagenesis: SEPM Special Publication 26, p. 209-225.

Shinn, E. A., 1983, Tidal flat environment, *in* P. A. Scholle, D. G. Bebout, and C. H. Moore, eds., Carbonate depositional environments: AAPG Memoir 33, p. 171-210.

Siebert, R. M., G. K. Moncure, and R. W. Lahann, 1984, A theory of framework grain dissolution in sandstones, *in* D. A. McDonald and R. C. Surdam, eds., Clastic diagenesis: AAPG Memoir 37, p. 163-176.

Siegel, J., 1989, The lithology, environment of deposition, and diagenesis of the Shattuck Member of the Queen Formation (Guadalupian, Permian) at Central Corbin Queen Field, Lea County, New Mexico: Master's thesis, Texas A&M University, College Station, Texas, 159 p.

Silver, B. A., and R. G. Todd, 1969, Permian cyclic strata, northern Midland and Delaware Basins, west Texas and southeastern New Mexico: AAPG Bulletin, v. 53, p. 2223-2251.

Surdam, R. C., S. W. Boese, and L. J. Crossey, 1984, The chemistry of secondary porosity, *in* D. A. McDonald and R. C. Surdam, eds., Clastic diagenesis: AAPG Memoir 37, p. 99-110.

Surdam, R. C., L. R. Crossey, E. Sven Hagen, and H. P. Heasler, 1989, Organic-inorganic interactions and sandstone diagenesis: AAPG Bulletin, v. 73, p. 1-23.

Tait, D. B., J. L. Allen, A. Gordon, G. L. Scott, W. S. Motts, and M. E. Spitler, 1962, Artesia Group of New Mexico and west Texas: AAPG Bulletin, v. 46, p. 504-517.

Walker, T. R., 1976, Diagenetic origin of continental red beds, *in* H. Falke, ed., The continental Permian in central, west, and south Europe: Dordrecht, Reidel, p. 240-282.

Ward, R.F., G. C. St. C Kendall, and P. M. Harris, 1986, Upper Permian (Guadalupian) facies and their association with hydrocarbons–Permian Basin, west Texas and New Mexico: AAPG Bulletin, v. 70, p. 239-262.

Warren, J. K., and C. G. St. C. Kendall, 1985, Comparison of sequences formed in marine sabkha (subaerial) and salina (subaqueous) settings–modern and ancient: AAPG Bulletin, v. 69, p. 1013-1023.

Warren, J. K., 1989, Evaporite sedimentology: importance in hydrocarbon accumulation: Englewood Cliffs, New Jersey, Prentice Hall, 285 p.

Warren, J. K., 1991, Sulfate dominated sea-marginal and platform evaporite settings: sabkhas and salinas, mudflats and salterns, *in* J. L. Melvin, ed., Evaporites, petroleum and mineral resources: Developments in sedimentology 50, p. 69-187.

Wheeler, C., 1989, Stratigraphy and sedimentology of the Shattuck Member (Queen Formation) and lowermost Seven Rivers Formation (Guadalupian), North McKittrick and Dog Canyons, Guadalupe Mountains, New Mexico and west Texas, *in* P. M. Harris, and G. A. Grover, eds., Subsurface and outcrop examination of the Capitan shelf margin, northern Delaware Basin: SEPM Core Workshop 13, p. 353-364.

Williams, K. W., 1967, Depositional dynamics of the Queen Formation, New Mexico and Texas, Master's thesis, Texas Tech University, Lubbock, Texas, 107 p.

Yang, K., and S. L. Dorobek, 1995a, The Permian Basin of west Texas and New Mexico: flexural modeling and evidence for lithospheric heterogeneity across the Marathon foreland, *in* S. L. Dorobek, and G. Ross, eds., Stratigraphic evolution of foreland basins: SEPM Special Publication 52, p. 37-62.

APPENDIX A

PRODUCTION DATA

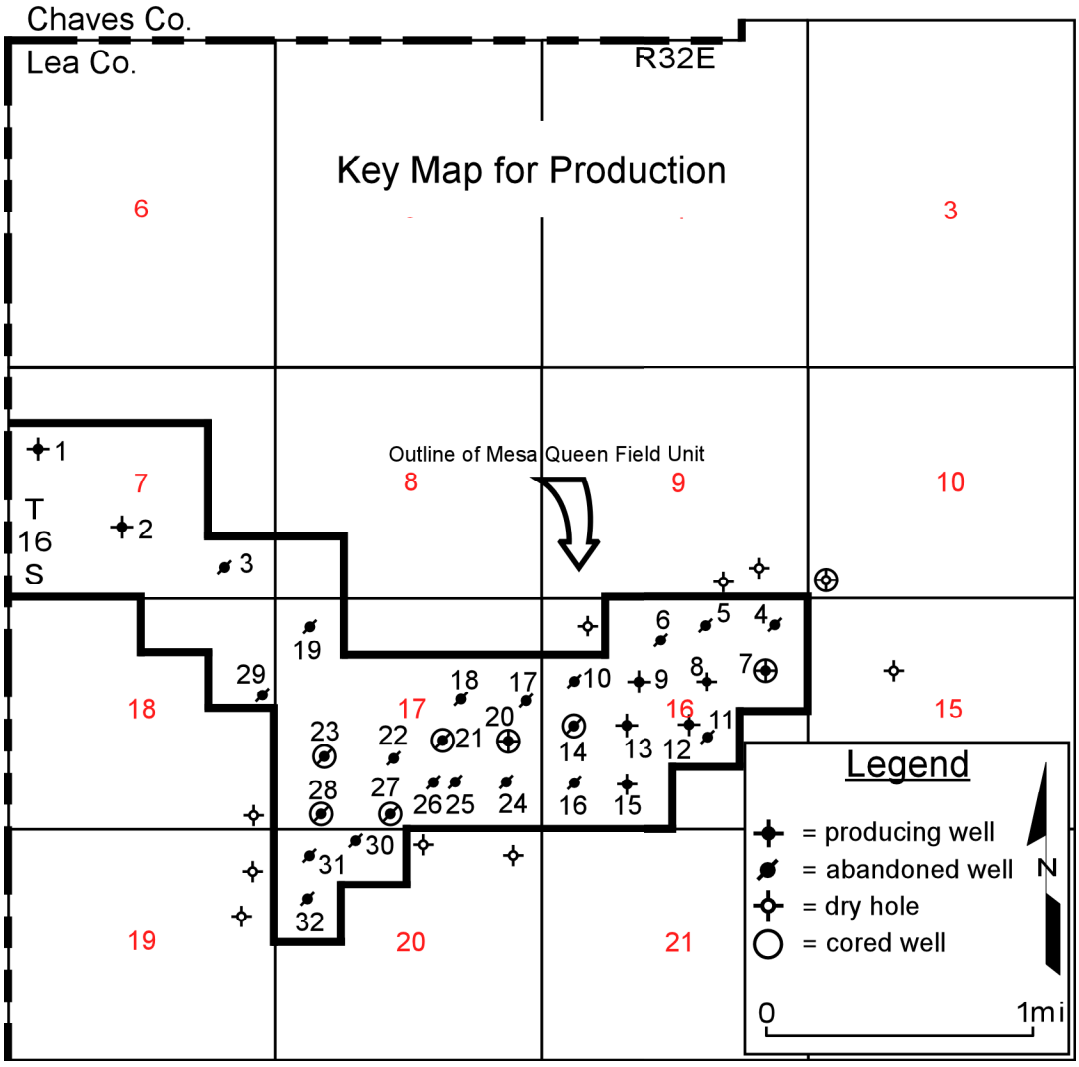
Chaves Co.
Lea Co.
R32E
Key Map for Production
Outline of Mesa Queen Field Unit
T
16
S
6
3
7
8
9
10
18
17
16
15
19
20
21
Legend
= producing well
= abandoned well
= dry hole
= cored well
N
0
1mi

Well #	Well Name	Section	Cum. Gas (mmcf)	Cum. Oil (bbl)
1	Mobil St. 7 #1	7	3167	4486
2	Pan Am St. 7 #1	7	1320	0
3	MQ 7 #1	7	182	0
4	Sinclair St. #2	16	68	161,959
5	Sinclair St. #1	16	69	45,759
6	Continental St. #1	16	41	99
7	MQ #1-A	16	36	39,679
8	Mobil St. #3	16	120	129,179
9	Mobil St. #1-B	16	359	203,490
10	Mobil St. #1	16	392	41,343
11	New Mexico St. BT	16	0	3256
12	Humble St. #1	16	16	7437
13	Mobil St. #4	16	229	228,334
14	MQ #1	16	188	247510
15	MQ 1-25	16	injector	injector
16	Sinclair St #3-A	16	94	48,334
17	Sinclair St. #1-A	17	383	27,344
18	Sinclair St. #2-A	17	428	26,569
19	Tidewater St. #1	17	969	204
20	MQB #1	17	93	135,531
21	MQC #1	17	340	78,822
22	MQD #2	17	211	35,885
23	MQD #4	17	334	1082
24	Mobil St. C	17	38	37,080
25	Continental St. B-2	17	226	39,890
26	Continental St. B-1	17	0	389
27	MQD #1	17	266	37,910
28	MQD #3	17	72	18,602
29	Sinclair St. A-1	18	383	27,344
30	State AT #1	20	34	48,793
31	DeCleva St. #1	20	4.7	40,107
32	Mesa Gulf #1	20	5.7	8,225

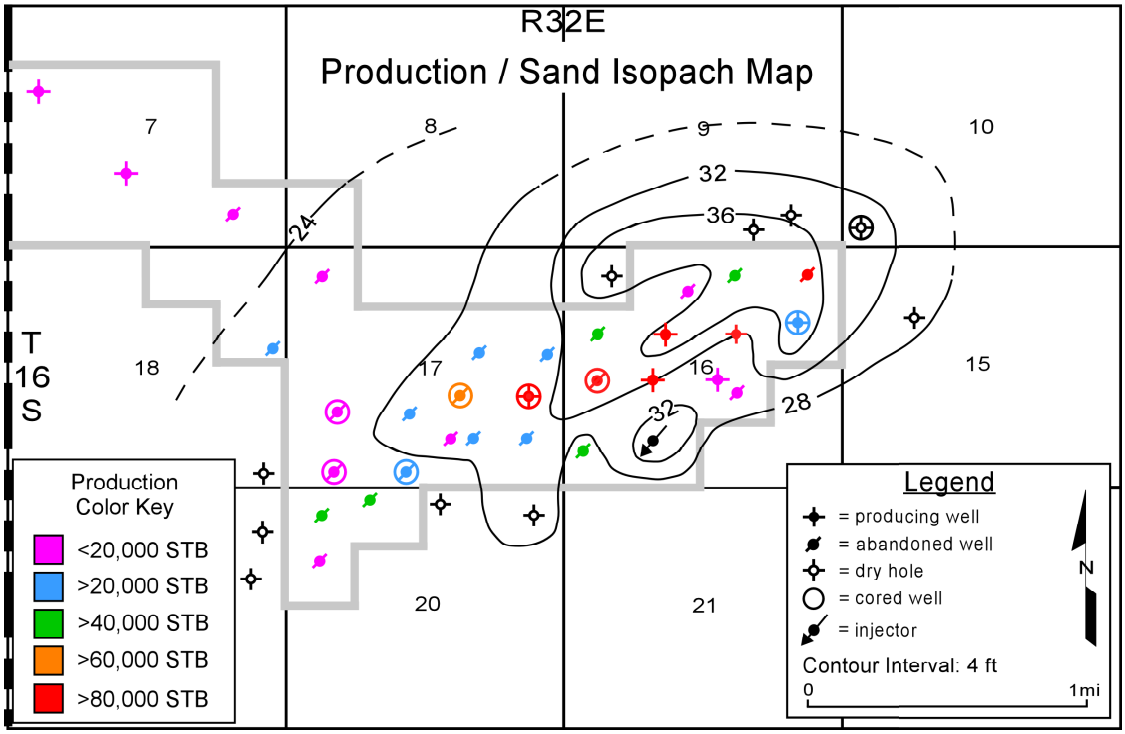
R32E
Production / Sand Isopach Map
7
8
9
10
T
16
S
18
17
16
15
20
21
24
32
36
28
32
Production
Color Key
<20,000 STB
>20,000 STB
>40,000 STB
>60,000 STB
>80,000 STB
Legend
= producing well
= abandoned well
= dry hole
= cored well
= injector
Contour Interval: 4 ft
0
1mi
N

APPENDIX B

LITHOSTRATIGRAPHIC COLUMNS

Lithology

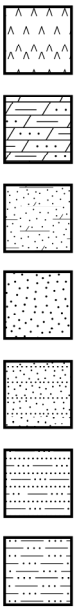

Bedded Anhydrite

Silty Dolomite

Dolomitic Sandstone

Massive Sandstone

Bedded/Laminated Sandstone

Interbedded Sandstone and Siltstone

Interbedded Siltstone and Mudstone

Bedding Contacts

- - - - Gradational

——— Sharp, Planar

Sharp, Wavy

—?— Missing/Unknown

Sedimentary Structures

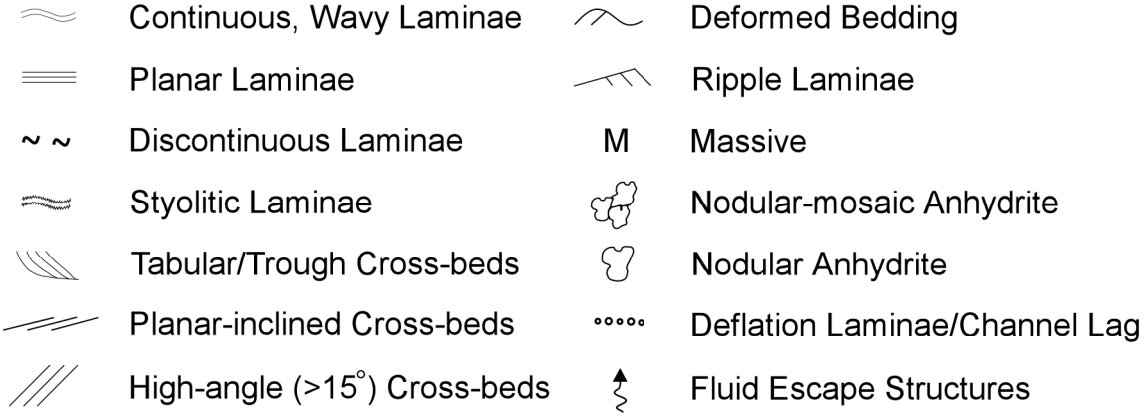

Continuous, Wavy Laminae

Planar Laminae

~ ~ Discontinuous Laminae

Styolitic Laminae

Tabular/Trough Cross-beds

Planar-inclined Cross-beds

High-angle (>15°) Cross-beds

Deformed Bedding

Ripple Laminae

M Massive

Nodular-mosaic Anhydrite

Nodular Anhydrite

Deflation Laminae/Channel Lag

Fluid Escape Structures

Alco State #1

Well Name: Alco St. #1
Location: Sec. 10, T16S, R32E
Cored Interval: 3358 -3405 (ft)

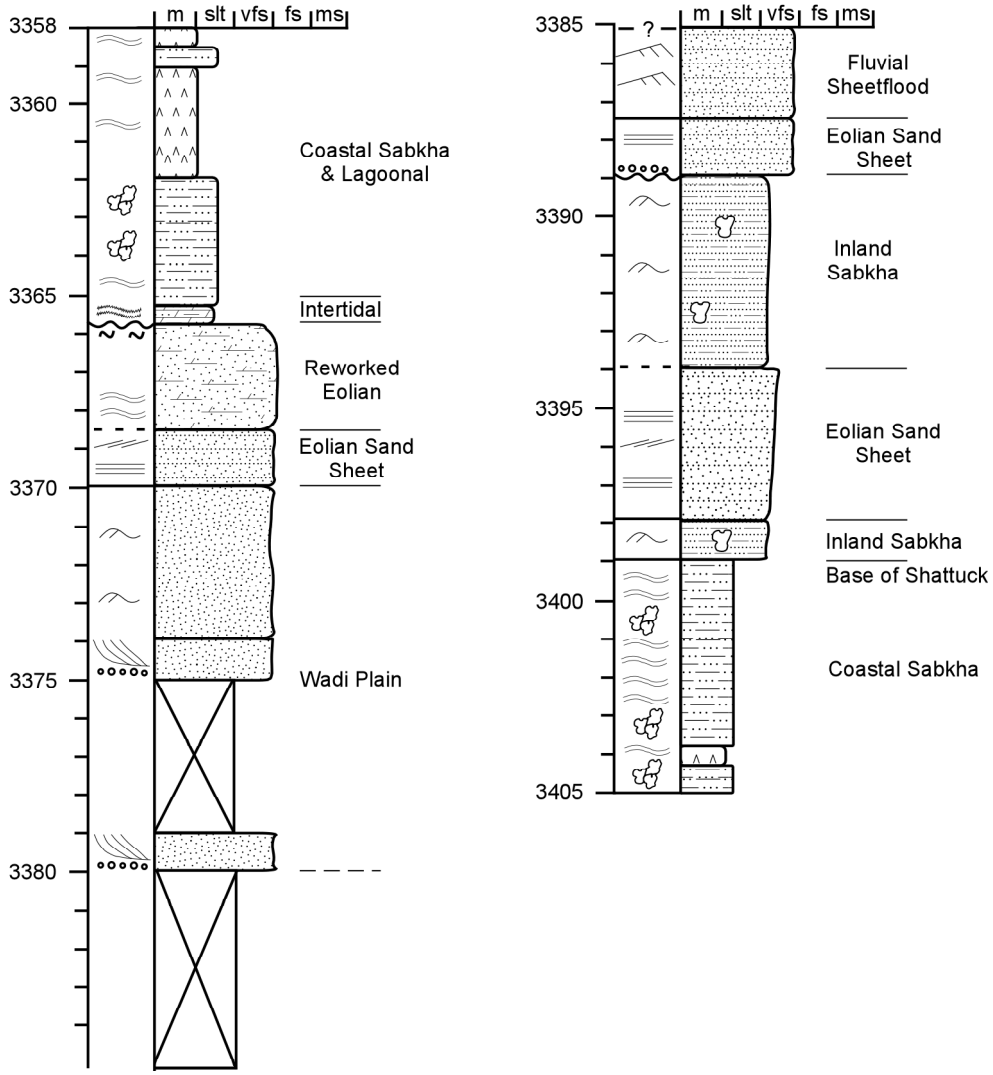

MQ #1 LITHOCOLUMN

Well Name: MQ #1
Location: Sec. 16, T16S, R32E
Cored Interval: 3400 - 3440 (ft)

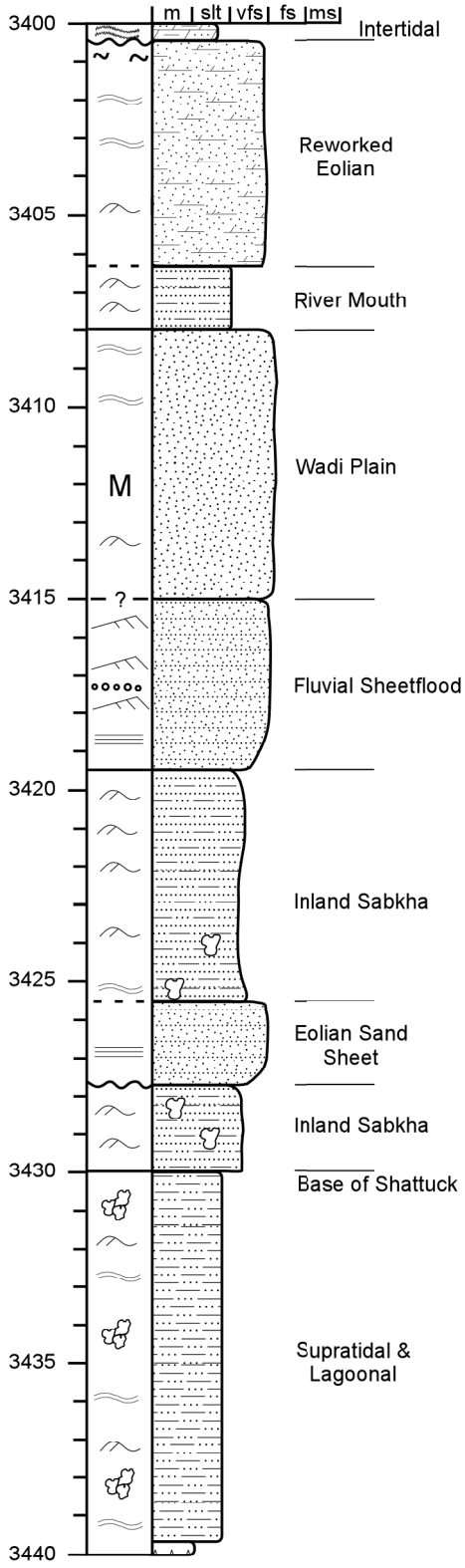

MQB #1 LITHOCOLUMN

Well Name: MQB #1
Location: Sec. 17, T16S, R32E
Cored Interval: 3384 - 3431 (ft)

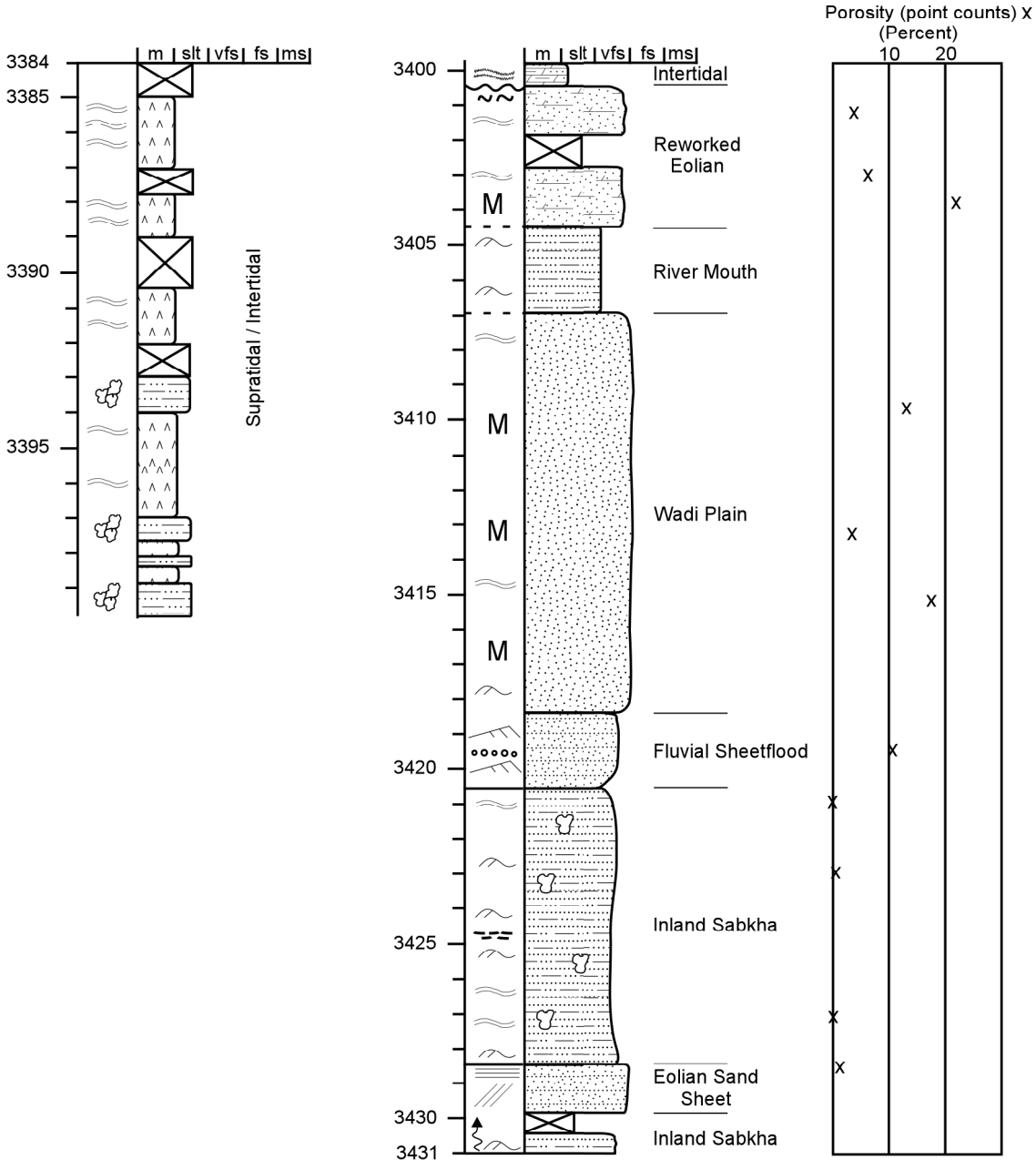

MQC #1 LITHOCOLUMN

Well Name: MQC #1
Location: Sec. 17, T16S, R32E
Cored Interval: 3397 - 3429 (ft)

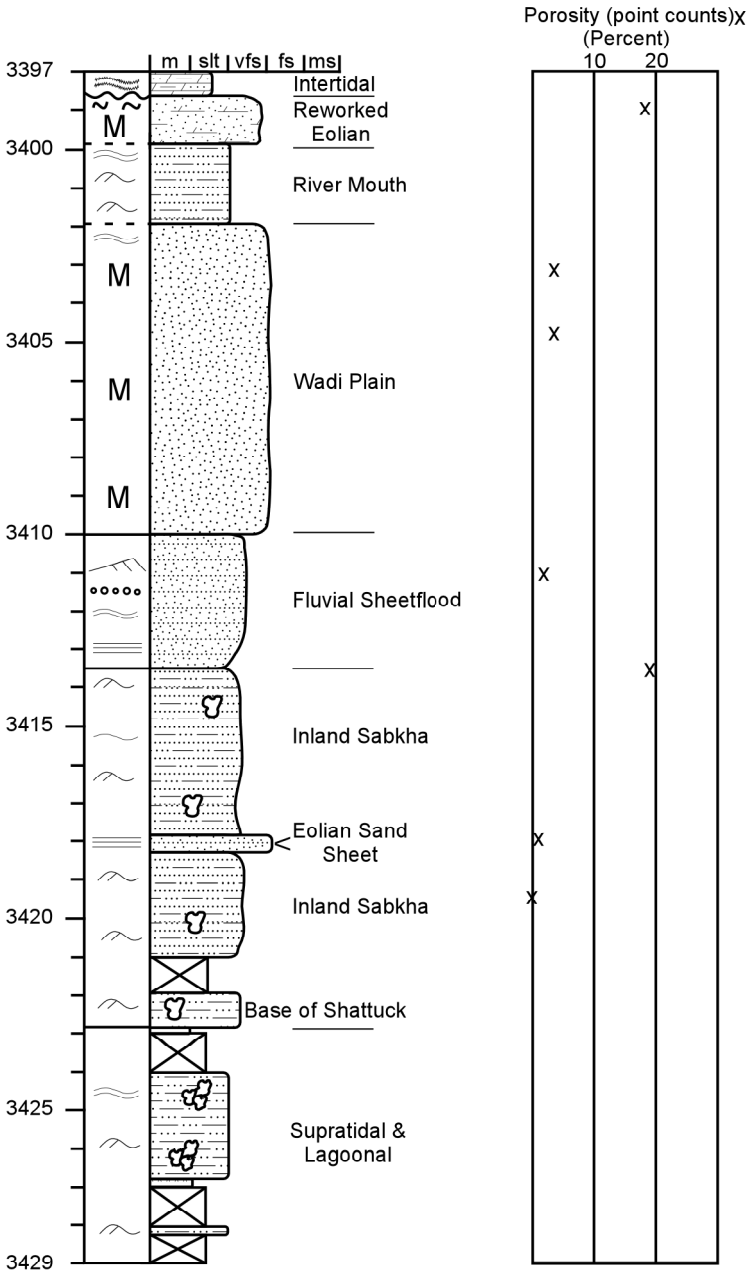

MQD #1 LITHOCOLUMN

Well Name: MQD #1
Location: Sec. 17, T16S, R32E
Cored Interval: 3362 - 3406 (ft)

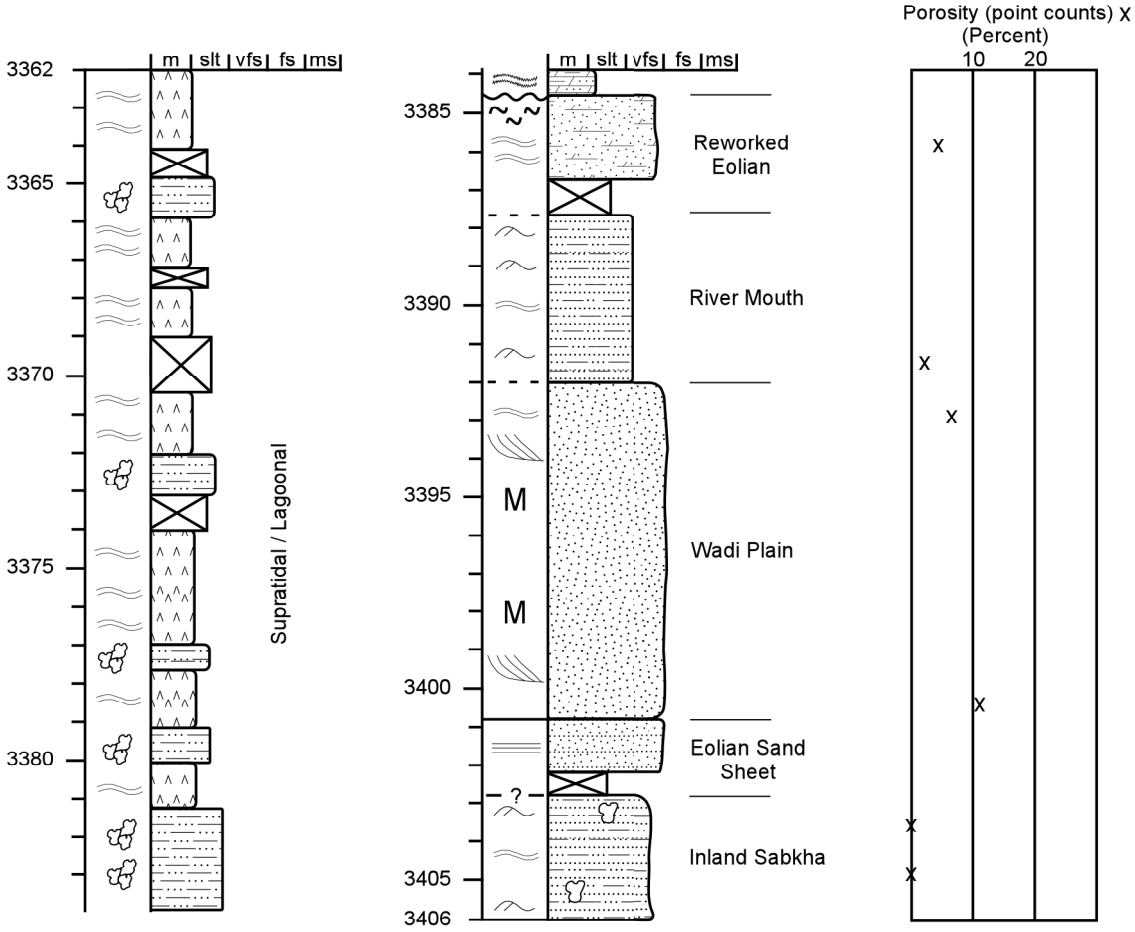

MQD #3 LITHOCOLUMN

Well Name: MQD #3
Location: Sec. 17, T16S, R32E
Cored Interval: 3375 - 3413 (ft)

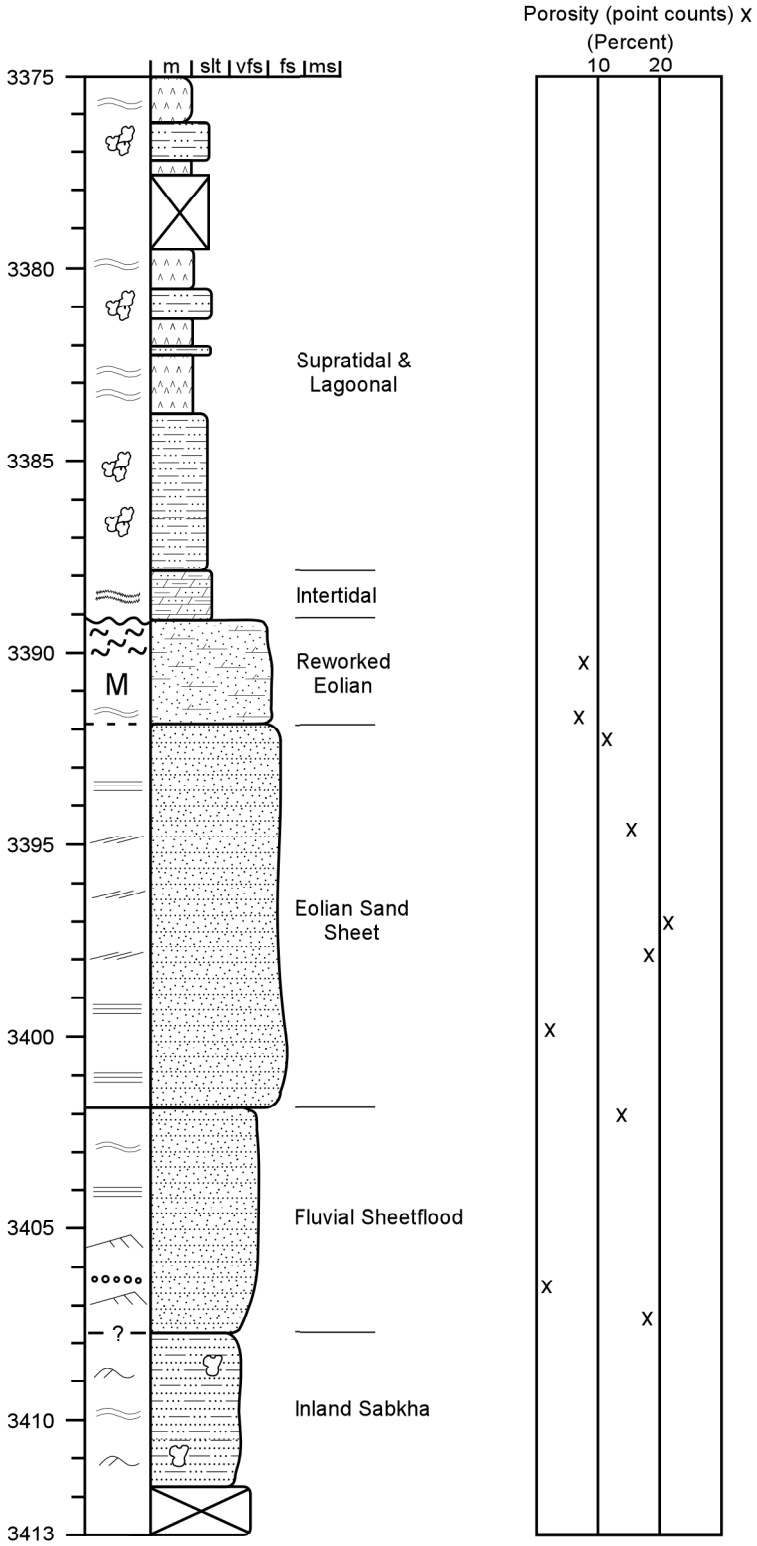

MQD #4 LITHOCOLUMN

Well Name: MQD #4
Location: Sec. 17, T16S, R32E
Cored Interval: 3365 -3400 (ft)

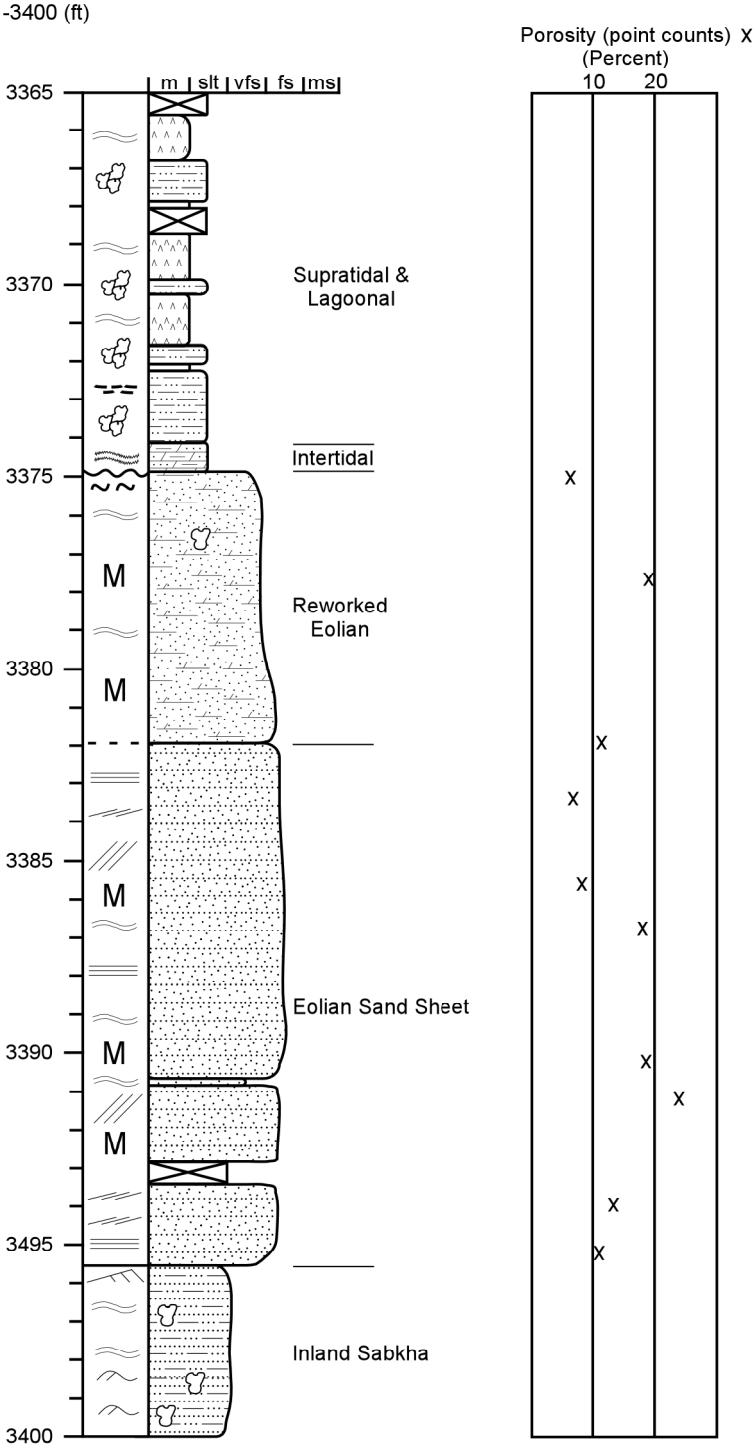

VITA

Name:	Jared Brandon Haight
Education:	Bachelor of Science, Geology The University of Oklahoma, Norman, OK 73019 December 1998
Professional Affiliations:	American Association of Petroleum Geologists Society of Economic Paleontologists and Mineralogists
Professional Experience:	Kerr-McGee Oil and Gas Corporation, Summer 2000
Permanent Address:	c/o Debbie Haight Box 195 Tyrone, OK 73951